



**HAL**  
open science

## Reduced obesity, diabetes and steatosis upon cinnamon and grape pomace are associated with changes in gut microbiota and markers of gut barrier

Matthias van Hul, Lucie Geurts, Hubert Plovier, Céline Druart, Amandine Everard, Marcus Ståhlman, Moez Rhimi, Kleopatra Chira, Pierre Louis Teissedre, Nathalie M. Delzenne, et al.

### ► To cite this version:

Matthias van Hul, Lucie Geurts, Hubert Plovier, Céline Druart, Amandine Everard, et al.. Reduced obesity, diabetes and steatosis upon cinnamon and grape pomace are associated with changes in gut microbiota and markers of gut barrier. *AJP - Endocrinology and Metabolism*, 2018, 314 (4), pp.E334-E352. 10.1152/ajpendo.00107.2017 . hal-02626402

**HAL Id: hal-02626402**

**<https://hal.inrae.fr/hal-02626402v1>**

Submitted on 26 May 2020

**HAL** is a multi-disciplinary open access archive for the deposit and dissemination of scientific research documents, whether they are published or not. The documents may come from teaching and research institutions in France or abroad, or from public or private research centers.

L'archive ouverte pluridisciplinaire **HAL**, est destinée au dépôt et à la diffusion de documents scientifiques de niveau recherche, publiés ou non, émanant des établissements d'enseignement et de recherche français ou étrangers, des laboratoires publics ou privés.



Distributed under a Creative Commons Attribution 4.0 International License

1 **Reduced obesity, diabetes and steatosis upon cinnamon and grape pomace**  
2 **are associated with changes in gut microbiota and markers of gut barrier**

3 Matthias Van Hul<sup>1</sup>, Lucie Geurts<sup>1</sup>, Hubert Plovier<sup>1</sup>, Céline Druart<sup>1</sup>, Amandine  
4 Everard<sup>1</sup>, Marcus Ståhlman<sup>2</sup>, Moez Rhimi<sup>3</sup>, Kleopatra Chira,<sup>6,7</sup> Pierre-Louis  
5 Teissedre<sup>6,7</sup>, Nathalie M. Delzenne<sup>1</sup>, Emmanuelle Maguin<sup>3</sup>, Angèle Guilbot<sup>4</sup>,  
6 Amandine Brochot<sup>4#</sup>, Philippe Gérard<sup>#3</sup>, Fredrik Bäckhed<sup>#2,5</sup>, Patrice D. Cani<sup>1\*</sup>

7  
8 <sup>1</sup> Université catholique de Louvain, Louvain Drug Research Institute, WELBIO  
9 (Walloon Excellence in Life sciences and BIOTEchnology), Metabolism and  
10 Nutrition research group, Brussels, Belgium,

11 <sup>2</sup> Wallenberg Laboratory, University of Gothenburg, Gothenburg, Sweden

12 <sup>3</sup> Micalis, INRA, AgroParisTech, Université Paris-Saclay, 78350, Jouy-en-Josas,  
13 France.

14 <sup>4</sup> Groupe PiLeJe, 75015, Paris, France.

15 <sup>5</sup> Novo Nordisk Foundation Center for Basic Metabolic Research, Section for  
16 Metabolic Receptology and Enteroendocrinology, Faculty of Health Sciences,  
17 University of Copenhagen, Copenhagen, Denmark.

18 <sup>6</sup> Univ. Bordeaux, ISVV, EA 4577 Œnologie, F-33140 Villenave d'Ornon, France

19 <sup>7</sup> INRA, ISVV, USC 1366 Œnologie, F-33140 Villenave d'Ornon, France

20  
21 # Equally contributed to this work

22  
23 \*Correspondence to: [Patrice.cani@uclouvain.be](mailto:Patrice.cani@uclouvain.be)  
24 Prof. Patrice D. Cani, Université catholique de Louvain, LDRI, Metabolism and  
25 Nutrition research group, Av. E. Mounier, 73 box B1.73.11, B-1200 Brussels,  
26 Belgium. Phone: +32 2 764 73 97

27 **Running title:** Cinnamon and grape extracts shape microbiota and metabolism

28 **Abstract**

29 Increasing evidence suggests that polyphenols have a significant potential in the  
30 prevention and treatment of risk factors associated with metabolic syndrome.  
31 The objective of this study was to assess the metabolic outcomes of two  
32 polyphenol-containing extracts from cinnamon bark (CBE) and grape pomace  
33 (GPE) on C57BL/6J mice fed a high-fat diet (HFD) for 8 weeks.

34 Both CBE and GPE were able to decrease fat mass gain and adipose tissue  
35 inflammation in mice fed a HFD without reducing food intake. This was  
36 associated with reduced liver steatosis and lower plasma non-esterified fatty  
37 acids levels. We also observed a beneficial effect on glucose homeostasis as  
38 evidenced by an improved glucose tolerance and a lower insulin resistance  
39 index.

40 These ameliorations of the overall metabolic profile were associated to a  
41 significant impact on the microbial composition, which was more profound for  
42 the GPE than for the CBE. At the genus level, *Peptococcus* were decreased in the  
43 CBE group. In the GPE treated group, several key genera that have been  
44 previously found to be linked with HFD, metabolic effects and gut barrier  
45 integrity were affected: we observed a decrease of *Desulfovibrio*, *Lactococcus*,  
46 whereas *Allobaculum* and *Roseburia* were increased.

47 In addition, the expression of several antimicrobial peptides and tight junction  
48 proteins was increased in response to both CBE and GPE supplementation,  
49 indicating an improvement of the gut barrier function.

50 Collectively, these data suggest that CBE and GPE can ameliorate the overall  
51 metabolic profile of mice on a high-fat diet, partly by acting on the gut  
52 microbiota.

## 53 Introduction

---

54 With more than one third of the adult population affected worldwide, obesity-  
55 associated metabolic disorders have become a major global health challenge that  
56 extends well beyond the developed world (1). Obesity is caused by a disparity  
57 between energy intake and energy expenditure, although genetic and  
58 environmental factors also influence this balance and modify metabolism (2).  
59 Obesity is associated with an excess of (white) adipose tissue mass, insulin  
60 resistance, liver fat accumulation, chronic pro-inflammatory state and major  
61 health issues that include a plethora of comorbidities, such as type 2 diabetes,  
62 cardiovascular diseases, hypertension, stroke, and certain types of cancer (3).  
63 Weight-reducing programs that recommend switching to a healthier lifestyle  
64 with reduced caloric intake and increased physical activity, although efficient,  
65 are difficult to maintain in the long term and therefore often remain unsuccessful  
66 (4). Unfortunately, available drugs are of limited efficacy and are associated with  
67 side effects (5). Plant extracts may represent an additional option in the support  
68 of weight management strategies (6).

69 Among these, polyphenols, a large family of compounds identified in plants, have  
70 attracted great interest because of their beneficial health effects (7). These  
71 effects are often attributed to their ability to relieve oxidative stress-induced  
72 tissue damage associated with chronic diseases via their antioxidant activity and  
73 free radical scavenging capacities. Interestingly, some polyphenols were shown  
74 to have anti-inflammatory and antimicrobial properties, thereby influencing the  
75 host gut microbiota, and eventually the inflammatory and metabolic status (8-  
76 12). In addition, we and others have demonstrated that the gut microbiota

77 contributes to the development of the metabolic disorders associated with  
78 obesity by modulating appetite (13, 14), energy harvest and absorption (14-16),  
79 gut motility, intestinal barrier function, inflammation (17, 18), glucose and lipid  
80 metabolism, as well as hepatic and adipose tissue fat storage (19). It was also  
81 reported that diets containing high fat levels diminish intestinal microbial  
82 diversity, often at the expense of more beneficial bacteria (20).

83 The aim of the present study was to determine the effects of two extracts of  
84 plants, cinnamon and grape pomace, known to be rich in polyphenols, in a mouse  
85 model of diet-induced obesity. Anti-diabetic and anti-inflammatory properties of  
86 cinnamon were reported in experimental studies (21-26) and the beneficial  
87 effects of grapes and grape by-products were documented in different aspects of  
88 the metabolic syndrome including dyslipidaemia, diabetes, hypertension, and  
89 obesity (27-29). However, only few studies have explored the impact of dietary  
90 polyphenols on the gut microbiota and intestinal barrier functions (28, 30-32),  
91 and many aspects of this interaction remain largely unknown. This assessment  
92 was therefore one of the main objectives of this study.

93

## 94 **Materials and Methods**

---

### 95 **Extracts**

96 The cinnamon bark extract (CBE), ChalCinn<sup>®</sup>, (3inature, Saint-Bonnet-de-  
97 Rochefort, France) was extracted from *Cinnamomum cassia*, rich in polyphenol  
98 type-A polymers (oligomeric proanthocyanidins)(21, 33).

99 The grape (*Vitis vinifera L.*) pomace extract (GPE) was supplied by 3iNature and  
100 sourced from Alicante from red wine cultivar in the Rhône valley. Grape pomace  
101 is a wine by-product that is characterized by high contents of phenolic

102 compounds due to an incomplete extraction during the winemaking process. It is  
103 a mixture of grape skins and seeds in near-equivalent amounts together with a  
104 small amount of stems (<6 %). The main polyphenols of grape pomace are  
105 anthocyanins, hydroxycinnamic acids, flavanols and flavanol glycosides (34).  
106 Extraction was performed with ethanol/water (30:70 v/v) at 85 °C and the  
107 extract was concentrated and vacuum-dried on non-extracted grape pomace.  
108 The final product thus consisted of Alicante grape pomace enriched with its own  
109 polyphenols.

110

### 111 **Reagents and Standards**

112 Deionized water was purified with a Milli-Q water system (Millipore, Bedford,  
113 MA, USA). HPLC grade acetonitrile, ethyl acetate, chloroform, methanol, ethanol  
114 and acetone purchased from Scharlau (Sentmenat, Barcelona, Spain). The  
115 following chemicals were obtained from Sigma Aldrich (St. Louis, MO, USA): (+)-  
116 catechin, (-)-epicatechin, B1 [(-)-epicatechin-(4 $\beta$ -8)-(+)-catechin], procyanidin  
117 dimer B2 [(-)-epicatechin-(4 $\beta$ -8)-(-)-epicatechin], cyanidin-3-O-glucoside  
118 chloride, delphinidin-3-O-glucoside chloride, malvidin-3-O-glucoside chloride,  
119 peonidin-3-O-glucoside chloride, gallic acid.

120 The Laboratory of Organic Chemistry and Organometallic (Université Bordeaux  
121 1) synthesized procyanidins dimers B3 [(+)-catechin-(4 $\alpha$ -8)-(+)-catechin], B4  
122 [(+)-catechin-(4 $\alpha$ -8)-(-)-epicatechin] and a trimer (C1) [(+)-catechin-(4 $\beta$ -8)-(+)-  
123 catechin-(4 $\beta$ -8)-(-)-epicatechin] (Tarascou et al., 2006).

124

125

### 126 **Grape pomace extract analysis**

## 127 **Tannins Extraction**

128 GPE (1 gr of dry matter) was solubilized in water/ethanol (250 mL, 95:5, v/v)  
129 and partitioned three times with chloroform (250 mL) to remove lipophilic  
130 material. The aqueous phase was then extracted three times with ethyl acetate  
131 (250 mL) to obtain two distinctive fractions: a low molecular weight procyanidin  
132 fraction (monomeric/oligomeric tannins) in the organic phase and a high weight  
133 procyanidin fraction (polymeric tannins) in the aqueous phase. These two  
134 fractions were concentrated and lyophilized.

135

## 136 **Anthocyanins Extraction**

137 Anthocyanin extraction was adapted from the method of Sriram et al. (1999).  
138 GPE (1 g) was extracted four times with acidified methanol (40 mL, 0.1% HCl  
139 12N) successively for 4 h, 12 h, 4 h and 12 h. The centrifugal supernatants were  
140 combined and evaporated in vacuo at 30 °C to remove methanol; the residue was  
141 dissolved in water and lyophilized to obtain an anthocyanin-rich powder.

142

## 143 **Total Phenolics and Tannins, Anthocyanins**

144 Total polyphenol contents (TPC) were determined in GPE and cinnamon bark  
145 extract (CBE). Tannin and anthocyanin contents were determined only in GPE.  
146 Crude extracts were solubilized in water/ethanol (90:10, v/v; pH 3.5 with  
147 tartaric acid) at appropriate concentrations. TPC was determined by the Folin-  
148 Ciocalteu assay [Singleton et al., 1965] and the data expressed as mg of gallic acid  
149 equivalents (GAE) per g dry weight. Total tannin content was measured by acidic  
150 hydrolysis using the method of Ribereau-Gayon and Stonestreet [Ribéreau et al.,

151 1966]. Anthocyanin content was determined by the SO<sub>2</sub> bleaching procedure  
152 [Ribéreau et al., 1965].

153

#### 154 **HPLC Analysis of Anthocyanins in GPE**

155 GPE was dissolved in water/methanol solution (50:50, v/v) at a concentration of  
156 10 mg/mL prior to UPLC-UV analyses using a Thermo-Accela HPLC system  
157 (Thermo-Fisher, San Jose, CA, USA) composed of a PDA detector, an autosampler  
158 and a quaternary 600 series pump system controlled by an Xcalibur data system.

159 Separation was performed on a C18 Kinetex column (100 mm × 2.1 mm, 1.7 μm).

160 The injected volume was 2 μL. The mobile phase pumped at 200 μL/min

161 comprised a 20 min, 7%–26% gradient of acetonitrile in water with both

162 solvents containing 5% formic acid. Eluting peaks were monitored at 520 nm.

163 Identification of main peaks was performed by comparison to external

164 standards (Anthocyanins monoglucosides (cyanidin-3-O-glucoside, delphinidin-3-

165 O-glucoside, paeonidin-3-O-glucoside, malvidin-3-O-glucoside, petunidin-3-O-

166 glucoside), acylated anthocyanins (paeonidin-3-O-glucoside, malvidin-3-O-

167 glucoside) and coumaroylated (paeonidin-3-O-glucoside, malvidin-3-O-

168 glucoside). The data was expressed as Malvidin-3-O-glucoside equivalent/g dry

169 weight GPE. (Ky et al., 2014).

170

#### 171 **Determination of Individual Tannins in GPE by HPLC Analysis**

172 GPE extract was solubilized in a methanol/water solution (50:50, v/v) at

173 appropriate concentrations and analyses of monomeric/oligomeric tannins

174 (catechin, epicatechin, dimers B1, B2, B3, B4 ; Trimer C2) were carried out



175 according to the method of Silva et al. [Silva et al, 2012]. The data was expressed  
176 as catechin equivalent/g dry weight GPE.

177

### 178 **Determination of Mean Degree of Polymerization (mDP) in GPE**

179 The proanthocyanidin mean degree of polymerization (mDP) was determined  
180 for GPE in monomeric/oligomeric and polymeric tannin fractions by the means  
181 of phloroglucinolysis [Drinkine et al., 2007]. Analyses were carried out using the  
182 same method as described by Lorrain et al. [Lorrain et al., 2011].

183 The oligomeric and polymeric proanthocyanidins were depolymerised in the  
184 presence of a nucleophilic agent phloroglucinol in an acidic medium. Reversed-  
185 phase HPLC analysis of the products formed allows determination of the  
186 structural composition of proanthocyanidins, which are characterised by the  
187 nature of their constitutive extension units (released as flavan-3-ols  
188 phloroglucinol adducts) and terminal units (released as flavan-3-ols). To  
189 calculate the apparent mDP, the sum of all subunits (flavan-3-ol monomer and  
190 phloroglucinol adducts, in mols) was divided by the sum of all flavan-3-ol  
191 monomers (in mols). GPE sample was analysed with a Surveyor series  
192 instrument (Thermo-Finnigan, Les Ullis, France) equipped with a 100 x 4.6 mm  
193 i.d., 3.5 µm X-Terra reversed-phase C18 column (Waters) thermostated at  
194 25°C. Detection was carried out at 280 nm using a Finnigan Surveyor PDA Plus  
195 detector. The mass detection was carried out using a Finnigan LCQ DECA XP MAX  
196 mass spectrometer with an ESI interface, performed in positive mode with the  
197 following parameters: capillary temperature 325 °C, capillary voltage 4 V,  
198 nebulizer gas flow 1.75 L/min, desolvation gas flow 1 L/min, and spray voltage 5  
199 kV. The solvents used were solvent A: H<sub>2</sub>O/AcOH (99:1 v/v), and B: MeOH. The

200 gradient consisted of 5% B during 25 min, linear gradient 5%–20% B in 20 min,  
201 then 20%–32% B in 15 min, finally 32%–100% B in 2 min. The column was  
202 washed with 100% B for 5 min and then stabilized with the initial conditions for  
203 10 min. The injection volume was 20 µL. The flow rate was 1 mL/min.

204

## 205 **Cinnamon bark extract analysis**

### 206 **Total proanthocyanidins**

207 In CBE, total proanthocyanidin content (PAC) was determined in EP using the  
208 BL-DMAC method as previously described (Lee et al., 2009) and quantified as A-  
209 type proanthocyanidin equivalents.

210

### 211 **Determination of essential oil in CBE**

212 CBE was ground and submitted to steam distillation (20,0 g of dried material) for  
213 8 h, using a Clevenger-type apparatus without hexane at a rate of 3-4 ml/min,  
214 according European Pharmacopoeia. The volatile distillates were analyzed by  
215 GC-MS. The ratio of CBE and water (acidified by 2 ml HCL 37% m/m) was 1:10.  
216 The essential oils were stored in amber vials at 4°C until analysis. The yield oil  
217 were kept frozen at temperature -20°C up to their utilization.

218 The essential oil were analysed on a Agilent gas chromatograph Model 7890,  
219 coupled to a Agilent MS model 5975 coupled to a computer equipped with  
220 Chemstation, equipped with a DB5 MS column (40m X 0.18mm, 0.18µm),  
221 programming from 50°C (5 min) to 300°C at 5°C/min, 5 min hold. Helium as  
222 carrier gas (1.0 ml/min); injection in split mode (1:80) ; injector, 280°C. The MS  
223 working in electron impact mode at 70 eV; electron multiplier, 1900 V; ion  
224 source temperature, 230°C ; mass spectra data were acquired in the scan mode

225 in  $m/z$  range 33-450. The essential oil is diluted in acetone: 1/100. The essential  
226 oil were analysed on a Agilent gas chromatograph Model 7890, equipped with a  
227 DB5 MS column (40m X 0,18mm, 0.18  $\mu\text{m}$ ), programming from 50°C (5 min) to  
228 300°C at 5°C/min, 5 min hold. Helium as carrier gas (1.0 ml/min); injection in  
229 split mode (1:80); injector and detector temperature, 280 and 300°C  
230 respectively. The essential oil is diluted in acetone: 1/100.

231 Components were identified by both GC retention times and by comparison of  
232 their mass with those present in the computer data bank and published spectra.  
233 Quantification was performed by area percent, FID-response factor = 1.

234

#### 235 **Determination of coumarin content in CBE**

236 About 3.0 g (accurately weighed to 0,0001 g) of powdered whole plant was  
237 extracted using 150 ml methanol R as solvent under reflux during 30 min. After  
238 filtration, the filtrate was adjusted to 250,0 ml with the same solvent. The sample  
239 were filtered using 0,45  $\mu\text{m}$  membrane filters (Millipore). Quantification of the  
240 constituent coumarin was carried out from the calibration curves of the HPLC  
241 chromatograms using authentic compounds. Coumarin (> 98%, HPLC)  
242 purchased from Sigma (St. Louis, MO, USA) was used as an external standard.

243 The coumarin content was determined according to reported methods [1] by an  
244 HPLC apparatus (Hitachi) consisting of a quaternary pump, a autosampler, and a  
245 Photodiode Array Detector (PDA). Separation was carried with a C18 column  
246 (4.6 mm x 250 mm) Purospher Star VWR. The column temperature was  
247 maintained at 25°C and the mobile phase flow rate at 1.5 ml/min. The mobile  
248 phase consisted of HPLC grade solvent Acetonitrile R and 5 g/L Phosphoric acid

249 (22:78 V/V). Coumarin content was quantified at 275 nm against the respective  
250 external standard.

251

## 252 **Mice**

253 Nine-week-old male C57BL/6J mice (Janvier, Le Genest-Saint-Isle, France) were  
254 housed in pairs in specific pathogen free conditions and in controlled  
255 environment (room temperature of  $23 \pm 2$  °C, 12 h daylight cycle) with free  
256 access to food and water. After an acclimatization period of one week, mice were  
257 randomly assigned to one of four dietary conditions (n = 14 per group). The  
258 different diets were as follow: control diet (CT) (10 kcal% fat, D12450Ji,  
259 Research Diet, New Brunswick, NJ, USA), high-fat diet (HFD) (60 kcal% fat,  
260 D12492i Research Diet), high-fat diet supplemented with 2 g cinnamon bark  
261 extract/kg (HFD-CBE) or a high-fat diet supplemented with 8.2 g grape pomace  
262 extract/kg (HFD-GPE) during 8 weeks. Body weight, food and water intake were  
263 recorded weekly. Body composition (lean and fat mass) was assessed by using  
264 7.5MHz time domain-nuclear magnetic resonance (TD-NMR) (LF50 Minispec,  
265 Bruker, Rheinstetten, Germany). In the final week of the experiment, feces were  
266 collected for each mouse and energy content was measured by calorimetric  
267 bomb analysis (Mouse Clinical Institute, Illkirch, France).

268 All mouse experiments were approved by and performed in accordance with the  
269 guidelines of the local ethics committee. Housing conditions were specified by  
270 the Belgian Law of May 29, 2013, regarding the protection of laboratory animals  
271 (agreement number LA1230314).

272

273

## 274 **Oral glucose tolerance test (OGTT)**

275 After 7 weeks of treatment, an oral glucose tolerance test (OGTT) was performed  
276 as previously described (35). Briefly, 6h-fasted mice were given an oral glucose  
277 load (2 g glucose per kg body weight) and blood glucose levels were measured at  
278 different time points: 30 min before and 15, 30, 60, 90 and 120 min after oral  
279 glucose load. Blood glucose was measured with a standard glucose meter (Accu  
280 Check, Roche, Basel, Switzerland) on blood samples collected from the tip of the  
281 tail vein.

282

## 283 **Insulin resistance index**

284 Plasma insulin concentration was determined using an ELISA kit (Mercodia,  
285 Uppsala, Sweden) according to the manufacturer's instructions. Insulin  
286 resistance index was determined by multiplying the area under the curve of both  
287 blood glucose (-30 to 120 min) and plasma insulin (-30 and 15 min) obtained  
288 following the oral glucose tolerance test (36). Glucose-induced insulin secretion  
289 was calculated as the difference between plasma insulin levels 30 min before and  
290 15 min after oral glucose load.

291

## 292 **Tissue sampling**

293 At the end of the treatment period (week 8), 9 animals from each group were  
294 anesthetized with isoflurane (Forene, Abbott, Queenborough, Kent, England) and  
295 blood was sampled from the portal and cava veins. After exsanguination, mice  
296 were killed by cervical dislocation. Subcutaneous adipose tissue depots,  
297 intestines, muscles and liver were precisely dissected, weighed and immediately  
298 immersed in liquid nitrogen followed by storage at -80°C for further analysis.

## 299 **Indirect calorimetry experiments**

300 The remaining mice ( $n = 5$  per group) were housed individually in specialized  
301 metabolic chambers (Phenomaster, TSE Systems GmbH, Bad Homburg,  
302 Germany) to measure whole energy expenditure, oxygen ( $O_2$ ) consumption and  
303 carbon dioxide ( $CO_2$ ) production, respiratory exchange ratio (RER, calculated as  
304  $vCO_2/vO_2$ ), food intake and spontaneous locomotor activity (36, 37). Activity was  
305 recorded using an infrared light beam-based locomotion monitoring system  
306 (expressed as counts per hour). Mice were allowed 48 h acclimatization before  
307 experimental measurements. After six days of measurements, mice were killed  
308 and tissues were sampled as described above.

309

## 310 **Histological analyses**

311 Subcutaneous adipose tissue depots were fixed in 4% paraformaldehyde for 24  
312 hours at room temperature. Samples were then immersed in ethanol 100 % for  
313 24 hours prior to processing for paraffin embedding.

314 To determine the adipocyte tissue diameter, paraffin sections of 8  $\mu m$  were  
315 stained with hematoxylin and eosin.

316 Macrophage infiltration in the adipose tissue was assessed by staining them with  
317 a MAC-2/galectin-3 antibody (CL8942AP, Cedarlane Laboratories, Burlington,  
318 Ontario, Canada) diluted 1:500 in blocking buffer overnight, and was detected  
319 with an anti-rat igG antibody (AI-4001, Vector Laboratories, Inc., Burlingame,  
320 California, USA) (10 mg/ml). Immune complexes were detected by the Dako  
321 Envision kit (Agilent Technologies, Santa Clara, California, USA) according to the  
322 manufacturer's instructions, and briefly counterstained with haematoxylin.

323 Hepatic lipid content was visualized by using Oil red O staining.

324 All analyses were performed in a blinded manner by the investigator and  
325 quantified using ImageJ software (Version 1.50a, National Institutes of Health,  
326 Bethesda, Maryland, USA). At least five high-magnification fields were selected at  
327 random for each mouse. Images were obtained using a SCN400 slide scanner and  
328 Digital Image Hub software (Leica Biosystems, Wetzlar, Germany).

329

### 330 **RNA preparation and Real-time qPCR analysis**

331 Total RNA was prepared from tissues using TriPure reagent (Roche).  
332 Quantification and integrity analysis of total RNA were performed by analyzing  
333 1 µl of each sample in an Agilent 2100 Bioanalyzer (Agilent RNA 6000 Nano Kit,  
334 Agilent, Santa Clara, California, USA). cDNA was prepared by reverse  
335 transcription of 1 µg total RNA using a Reverse Transcription System kit  
336 (Promega, Madison, Wisconsin, USA). Real-time PCR was performed with the  
337 CFX96 real-time PCR system and CFX Manager 3.1 software (Bio-Rad, Hercules,  
338 California, USA) using Mesa Fast qPCR (Eurogentec, Liège, Belgium) for detection  
339 according to the manufacturer's instructions. RPL19 was chosen as the  
340 housekeeping gene. All samples were performed in duplicate, and data were  
341 analyzed according to the  $2^{-\Delta\Delta CT}$  method. The identity and purity of the amplified  
342 product were assessed by melting curve analysis at the end of amplification. The  
343 primer sequences for the targeted mouse genes are presented in Table 1.

344

### 345 **Biochemical analyses**

346 Plasma adipokines (leptin, resistin) and inflammatory markers (IL1b, IFNg,  
347 MCP1, MIP1a, PAI1) were detected by using a Bio-Plex Milliplex kit (Millipore,  
348 Billerica, Massachusetts, USA) and their concentrations were measured by using

349 Luminex technology (Bio-Rad Bioplex; Bio-Rad) following the manufacturer's  
350 instructions.

351 Plasma non-esterified fatty acids, cholesterol and triglyceride concentrations  
352 were measured using kits coupling an enzymatic reaction with  
353 spectrophotometric detection of the reaction end-products (Diasys Diagnostic  
354 and Systems, Holzheim, Germany) according to the manufacturer's instructions.

355 Total lipids were measured in the liver tissue after extraction in CHCl<sub>3</sub>:MeOH  
356 according to Folch et al. (38) and adapted as follows: Briefly, 100 mg of liver  
357 tissue was homogenized in 2 ml of CHCl<sub>3</sub>:MeOH (2:1) using a Tissue Lyser  
358 followed by an ultrasonic homogenizer. 400 µl of 0.9% NaCl solution was added  
359 and lipids were then extracted by vigorous shaking. After centrifugation, the  
360 lipidic phase was recovered in glass tubes and dried under a stream of N<sub>2</sub>. Glass  
361 tubes were weighed before and after lipid extraction to quantify total lipid  
362 content. The dried residue was solubilized in 1.5 to 3 ml isopropanol depending  
363 on the lipid content.

364

### 365 **Short chain fatty acid (SCFA) measurements**

366 Short-chain fatty acids in cecal samples were analyzed by gas-liquid  
367 chromatography as described previously (39).

368

### 369 **Bile Acids (BA) measurements**

370 The extraction and analysis of bile acids were performed according to a previous  
371 work (40). Briefly, bile acids from portal vein plasma were extracted by protein  
372 precipitation with 10 volumes of IS-containing methanol. After the samples were  
373 vortexed and centrifuged, the supernatant was diluted 50 times in



374 methanol:water (1:1). Bile acids from cecum (15-100 mg in 2 ml polypropylene  
375 tubes filled with ceramic beads) were extracted in 500µl IS-containing methanol  
376 using a TissueLyser II instrument (Retsch, Haan, Germany). The supernatant was  
377 diluted 50 times in methanol:water (1:1). Separation was performed using water  
378 and acetonitrile on a Kinetex C18 column (2.1 ×100 mm with 1.7 µm particles;  
379 Phenomenex, Torrance, California, USA). Detection was performed using a  
380 QTRAP 5500 instrument (AB Sciex, Toronto, Canada) with MRM in negative  
381 mode.

382

### 383 **Gut microbiota analysis**

384 The V3-V4 region was amplified from purified DNA with the primers F343  
385 (CTTTCCTACACGACGCTCTTCCGATCTACGGRAGGCAGCAG) and R784  
386 (GGAGTTCAGACGTGTGCTCTTCCGATCTTACCAGGGTATCTAATCCT) using 30  
387 amplification cycles with an annealing temperature of 65°C. The amplicon  
388 lengths were about 510 bp (the exact length varies depending on the species).  
389 Because MiSeq sequencing enables paired 250-bp reads, the ends of each read  
390 overlap and can be stitched together to generate extremely high-quality, full-  
391 length reads covering the entire V3-V4 region. Single multiplexing was  
392 performed using a home-made 6 bp index, which was added to the R784 primer  
393 during a second PCR with 12 cycles using the forward primer  
394 (AATGATACGGCGACCACCGAGATCTACTCTTTCCTACACGAC) and the  
395 modified reverse primer (CAAGCAGAAGACGGCATACGAGAT-index-  
396 GTGACTGGAGTTCAGACGTGT). The resulting PCR products were purified and  
397 loaded onto the Illumina MiSeq cartridge according to the manufacturer  
398 instructions. The quality of the run was checked internally using PhiX, and for

399 further analysis, each pair-end sequence was assigned to its sample using the  
400 previously integrated index.

401

#### 402 **Bioinformatics analysis**

403 Sequences were trimmed for adaptors and assembled with Flash1.6.2 (41). PCR  
404 primers were removed and sequences with sequencing errors in the primers  
405 were excluded (Mothur) (42). For each sample, 12000 reads were randomly  
406 selected for each sample. Chimera were removed with UCHIME (43) and Mothur  
407 (42) softwares. Reads were clustered into Operational Taxonomic Units (OTUs)  
408 at the 97% identity level using Esprit-tree (44). A reference sequence was picked  
409 for each OTU and assigned it at different taxonomic levels (from phylum to  
410 species) using the Greengenes database (release 13-5) (45) and the RDP  
411 classifier (46).

412

#### 413 **Statistical analysis**

414 Mouse data are expressed as the mean  $\pm$  SEM. Differences between groups were  
415 assessed using non-parametric Kruskal–Wallis one-way analysis of variance  
416 (ANOVA), followed by the Dunn’s multiple comparison test. Variance was  
417 compared using a Bartlett’s test. If variances were significantly different between  
418 groups, values were normalized by Log-transformation before proceeding to the  
419 analysis. When only two groups were compared, a non-parametric Mann-  
420 Whitney test was used. Regimen and treatment effects on community  
421 compositions were assessed using permutational multivariate analysis of  
422 variances (PERMANOVA) after rarefaction of all communities to even sampling  
423 depths. The abundances of all families were computed by agglomerating the

424 OTUs assigned to those families. For each such family, Mann-Whitney test with  
425 BH correction (47) were performed to detect the combinations (treatment) that  
426 were significantly different in terms of abundance. The same procedure was  
427 applied for each genus and for each OTUs. All analyses were done using R (R  
428 Core Team, 2015, R Foundation for Statistical Computing, Vienna, Austria)  
429 A two-way ANOVA analysis with a Bonferonni post-hoc test on repeated  
430 measurements was performed for the evolution of glycaemia and insulinemia  
431 during the OGTT. For all analyses and for each group, any exclusion decision was  
432 supported by the use of the Grubbs test for outlier detection.

## 433 Results

---

### 434 **Polyphenol content and profile of grape and cinnamon extracts**

435 GPE contained  $82.663 \pm 2.534$  mg/g total phenolics as gallic acid equivalents  
436 (GAE). Total anthocyanin and tannin contents of the GPE fraction were  $43.969 \pm$   
437  $3.497$  (as cyanidin-3-O-glucoside equivalent) and  $26.006 \pm 1.066$  (as procyanidin  
438 B2 equivalent), respectively, (Table 2). Individual anthocyanin analysis revealed  
439 that the most abundant anthocyanins present in GPE were malvidin-3-O-  
440 glucoside ( $21.594 \pm 0.213$  mg/g), peonidin-3-O-glucoside ( $8.687 \pm 0.258$  mg/g)  
441 and malvidin-3-O-(6''-p-coumaryl-glucoside) ( $4.624 \pm 0.012$  mg/g) (Table 2).  
442 The mean degree of polymerization of the proanthocyanidins in the GPE fraction  
443 was  $4.2 \pm 0.025$  (data not shown).

444 CBE contained 79 mg/g of total phenolics as GAE. Proanthocyanidin A content  
445 was 90 mg/g. Coumarin and cinnamaldehyde represented 9 mg/g and 1.8 mg/g  
446 respectively.

447

### 448 **Effects on body weight, body composition, adipose tissues and adipokines**

449 Body weight gain and fat mass gain were both significantly greater in all high-fat  
450 diet treated groups (HFD, HFD-CBE, HFD-GPE) than in mice fed the control diet  
451 (CT) (Fig 1A, B). Compared to the HFD-group, HFD-GPE ( $p = 0.03$ , 2-way  
452 repeated measurements ANOVA) and -CBE groups (trend,  $p = 0.1$ ) had a lower  
453 fat mass gain during the last 4 week of follow-up (Fig 1B, E, F) but no significant  
454 difference in body weight and lean mass gain were observed in the extract-  
455 treated groups (Fig 1A-F).

456 Brown and White adipose tissue depots were consistently smaller in the extract-  
457 treated groups compared to the HFD group, but there was no statistical  
458 difference (Fig 1G-I). These findings were mirrored by a trend in reduced leptin  
459 plasma levels in the HFD-GPE group ( $p = 0.08$  versus HFD, Mann-Whitney test)  
460 (Fig 1J).

461 The weights of liver, spleen and different muscles were not affected by the  
462 different diets (data not shown).

463

#### 464 **Effects on glucose homeostasis**

465 Both CBE and GPE treatments significantly improved glucose tolerance, as  
466 evidenced by a lower blood glucose profile compared to the untreated HFD-fed  
467 group (Fig 2A). The effect was stronger for the HFD-CBE group as evidenced by  
468 the significantly reduced area under the curve (Fig 2B).

469 Mice fed a HFD were hyperinsulinemic in the fasted state, as they exhibited more  
470 than two-fold higher levels of plasma insulin as compared to control mice (Fig  
471 2C). Mice from the HFD-GPE group produced somewhat less insulin in response  
472 to oral glucose administration compared to the HFD and HFD-CBE mice without  
473 reaching statistical significance (Fig 2C) ( $p = 0.07$  versus HFD, Mann-Whitney  
474 test). This result was corroborated by a decreasing trend for glucose-induced  
475 insulin secretion compared to the HFD and HFD-CBE groups ( $p = 0.08$  versus  
476 HFD, non-parametric Mann-Whitney test)(Fig 2D) and a significant improvement  
477 of the insulin resistance index (Fig 2E) in the HFD-GPE treated group. This was in  
478 accordance with a smaller adipocyte size (Fig 2F-G) and a trend in lower  
479 circulating resistin levels (Fig 2H), factors that have previously been associated  
480 with insulin resistance (37). For the HFD-CBE group no difference in glucose-

481 induced insulin secretion could be observed but there was a trend towards an  
482 improvement of the insulin resistance index compared to the HFD group ( $p =$   
483 0.06 versus HFD, Mann-Whitney test)(Fig 2E).

484

#### 485 **Effects on energy homeostasis**

486 The reduced fat mass gain observed in HFD-GPE mice could not be explained by  
487 any difference in energy intake (Fig 3A). On the contrary, there was a trend  
488 towards a higher mean calorie intake in HFD-GPE mice ( $p = 0.08$  versus HFD,  
489 Mann-Whitney test). HFD-GPE mice also had a significantly increased amount of  
490 feces excreted compared to the other HFD groups (Fig 3B). In addition, bomb  
491 calorimetric analysis of the different groups revealed a higher energy content in  
492 the fecal material of mice supplemented with cinnamon or grape extract (Fig 3C),  
493 resulting in higher daily energy excretion in both groups, as compared to HFD  
494 (Fig 3D). There was no difference when expressing this as percentage of the food  
495 intake (Fig3E).

496 The basal energy expenditure, which can also affect energy balance, was  
497 calculated by measuring the  $O_2$  consumption and the  $CO_2$  production for each  
498 mouse (not shown). After correction for the individual lean masses, the analysis  
499 revealed a mean increase in energy expenditure for the HFD, HFD-CBE and HFD-  
500 GPE groups, as compared to the CT group, without any effect of dietary  
501 supplementation (Fig 3F-G). In addition, body temperatures were not different  
502 between all four groups (Fig 3H). The respiratory exchange rate (RER) showed a  
503 clear metabolic shift from carbohydrate to lipid oxidation in the three HFD  
504 treated groups as compared to CT mice (Fig 3I).

505 Spontaneous physical activity (monitored by continuously counting the number  
506 of times a mouse crossed the different light beams in the metabolic cages) was  
507 increased in HFD-GPE mice in comparison with HFD mice ( $p = 0.02$  versus HFD,  
508 2-way repeated measurement ANOVA) (Fig 3J), whereas this effect was less  
509 pronounced in HFD-CBE mice ( $p = 0.18$ ).

510

### 511 **Effects on nutrients absorption**

512 To investigate the mechanism associated with reduced energy harvest, we  
513 measured different nutrient transporters in the proximal part of the intestines  
514 (jejunum) (Fig3K). Glucose transporters (Slc5a1/SGLT1, Slc2a2/GLUT2) were  
515 slightly lower in the high-fat fed group, whereas FABP1/LFABP and CD36, fatty  
516 acid binding proteins, are higher, confirming the switch from glucose  
517 consumption to lipid oxidation. Both CBE and GPE slightly increased SGLT1, but  
518 only GPE increased GLUT2 as well. LFABP was somewhat decreased by the GPE,  
519 as was CD36 by CBE. However, these changes were too subtle to achieve  
520 statistical significance.

521

### 522 **Effects on whole-body and hepatic lipid metabolism**

523 The management of dyslipidemia is a key element in the prevention of  
524 cardiovascular diseases in obese and diabetic patients. Therefore, we performed  
525 an analysis of circulating and liver lipids. Interestingly, circulating non-esterified  
526 fatty acids levels (NEFAs) were higher in the HFD group than in the control  
527 group and were normalized in the CBE and GPE treated groups although without  
528 reaching significance ( $p = 0.06$  and  $0.08$  versus HFD respectively, Mann-Whitney

529 test). Cholesterol plasma levels were increased in all HFD-treated groups,  
530 whereas circulating triglycerides were similar between groups (Fig 4A).  
531 In the liver, HFD increased the total lipid content by about 40%. Interestingly,  
532 treatment with GPE completely blunted this effect (Fig 4B). This was reflected by  
533 a significant normalization of liver triglyceride levels and a similar trend for  
534 cholesterol. In the HFD-CBE group, a trend for normalization was also observed  
535 for total lipid content and triglycerides, while cholesterol levels remained  
536 unaffected ( $p = 0.06$  versus CT,  $p = 0.6$  versus HFD, Mann-Whitney test). This  
537 finding was confirmed by the histological analysis that revealed significantly  
538 increased hepatic lipid depots in HFD mice, and smaller lipid droplets in the  
539 HFD-CBE and HFD-GPE mice (Fig 4C).

540

#### 541 **Effects on adipose tissue and systemic inflammation**

542 Diabetes and insulin resistance being frequently associated with adipose tissue  
543 inflammation (17, 48, 49), we measured various macrophage infiltration  
544 markers in the subcutaneous (SAT) and visceral adipose tissue (VAT) using qPCR  
545 analysis (Fig 5A and 5B, respectively). Integrin alpha X (ITGAX/CD11c),  
546 lipopolysaccharide binding protein (LBP) and monocyte chemoattractant  
547 protein-1 (MCP1) were upregulated by HFD and were reduced by GPE in both  
548 adipose tissues. CBE supplementation decreased CD11c and LBP, but not MCP1.  
549 Two other macrophage markers, F4/80 and CD68, were not differently  
550 expressed in any group (Fig 5A).

551 Histological analysis of the SAT stained with MAC2/Galectin-3, a marker of  
552 activated macrophages, showed a 2.5-fold higher number of macrophages in the  
553 HFD mice than in CT mice (Fig 5B), whereas this accumulation of macrophages



554 was markedly decreased in the HFD-CBE and HFD-GPE groups compared to the  
555 HFD group, although without reaching significance (Fig 5B).

556 To evaluate systemic inflammation, we measured circulating inflammatory  
557 markers in plasma (Fig 5D). We did not find a marked HFD effect for any of the  
558 markers, indicating that although there is a tissue inflammatory tone, they have  
559 not yet reached systemic inflammation. However, the GPE tended to be  
560 systematically lower than the other groups, especially for IFN $\gamma$  ( $p = 0,02$  versus  
561 HFD, Mann-Whitney test).

562

### 563 **Effects on gut microbiota**

564 We and others have previously linked the gut microbiota with low-grade  
565 inflammation and metabolic disorders associated with HFD feeding (17, 50-52).

566 The composition of the gut microbiota of mice that received HFD was  
567 significantly changed compared to those fed with CT diet, with an enrichment in  
568 Firmicutes and a decrease in Bacteroidetes (Fig 6A).

569 At the phylum level, no clear differences were observed in HFD-CBE mice when

570 compared to HFD. GPE treatment, however, increased the abundance of

571 Bacteroidetes at the expense of the Proteobacteria (Fig 6A). As observed in the

572 principal coordinates analysis (PCoA), HFD feeding caused a shift in microbiota

573 composition along the axis 1, explaining more than 57% of the difference

574 observed (Fig 6C). Conversely, most mice from the HFD-CBE and HFD-GPE

575 groups were separated from the untreated HFD-fed mice according to the axis 2.

576 At the operational taxonomic units (OTUs) level, this shift was modest in the

577 HFD-CBE group but more profound in the HFD-GPE group (Fig 6B). More

578 specifically, the abundance of 11 OTUs was significantly different in HFD-CBE

579 mice compared with HFD mice. In HFD-GPE mice, 53 OTUs were significantly  
580 modified (Fig 6B). Interestingly, the gut microbiota from extract-treated mice  
581 differed from that of the HFD mice but also from that of the CT mice, suggesting  
582 that polyphenols may have specific effects on the gut microbiota (Fig 6D).

583 At the family level, CBE supplementation significantly reduced the levels of  
584 *Peptococcaceae* (classified within the Firmicutes phylum) when compared to the  
585 HFD mice (Fig 6D, E). Supplementation with GPE reduced the levels of  
586 *Desulfovibrionaceae* and *Streptococcaceae*, while increasing the levels of  
587 *Prevotellaceae* and *Erysipelotrichaceae* (Fig 6D, E).

588 At the genus level, *Peptococcus* were decreased in the CBE group (Fig 6F). In the  
589 GPE treated group, we observed a decrease of *Desulfovibrio*, *Clostridium sensu*  
590 *stricto* and *Lactococcus*, whereas *Allobaculum* and *Roseburia* were increased (Fig  
591 6F).

592

### 593 **Effects on intestinal barrier**

594 HFD feeding and concomitant changes in the gut microbiota are linked to  
595 alterations in the intestinal gut barrier function and in the production of  
596 antimicrobial peptides. Here we found that HFD lowered the gene expression of  
597 the antimicrobial peptide Reg3 $\gamma$  all along the intestinal tract (Fig 7A and data not  
598 shown for jejunum and ileum) and lowered the expression of intectin, encoding a  
599 protein involved in the turnover of intestinal mucosa, in the colon (Fig 7B) and  
600 jejunum (data not shown).

601 In the colon, CBE tended to increase levels of intectin (Fig 7B) ( $p = 0.008$  versus  
602 HFD, Mann-Whitney test), of the antimicrobial peptides Lyz1 ( $p = 0.03$ ) (Fig 7F)  
603 and of the tight-junction protein claudin3 ( $p = 0.03$ ) (Fig 7E) compared to the

604 HFD group. Levels of the microbicidal protein Ang4 were higher in the HFD-CBE  
605 group as compared to CT mice (Fig 7G). HFD-GPE treatment normalized the  
606 levels of Reg3 $\gamma$  ( $p = 0.02$  versus HFD, Mann-Whitney test) (Fig 7A) in the colon  
607 and significantly increased the levels of Lyz1 (Fig 7F). The tight junction protein  
608 Occludin was somewhat higher in the treated groups when compared to CT and  
609 HFD mice, but this did not reach significance (Fig 7D). ZO-1 remained unaffected  
610 along the gastro-intestinal tract for all the HFD-treated groups (Fig 7C and data  
611 not shown).

612

### 613 **Effects on bile acids**

614 Primary bile acids (BAs) are synthesized by the liver and may be converted into  
615 secondary BAs as a result of biotransformation by the intestinal microbiota (53).  
616 They serve many important physiological functions, including glucose and lipid  
617 metabolism (54). HFD increased total BAs concentration in cecal content ( $p =$   
618  $0.03$  versus CT, Mann-Whitney test) and supplementation with CBE further  
619 increased cecal content in BAs compared to the HFD group (Fig 8A), although  
620 this did not reach statistical significance. Interestingly, this effect was due solely  
621 to an increase in conjugated BAs (Fig 8B), since unconjugated BAs levels did not  
622 differ between HFD groups (Fig 8C). At the level of individual BAs, we could not  
623 pinpoint one specific BA responsible for this increase; it was rather an  
624 accumulation of small changes throughout the BA spectrum that contributed to  
625 this overall increase (Fig 8D).

626 In portal vein plasma, total BA concentrations tended to be reduced in untreated  
627 HFD mice as compared to CT mice, but were higher in the HFD-CBE and HFD-  
628 GPE groups than in the HFD group, reaching levels comparable to that of the CT

629 group (Fig 8E). The percentage of conjugated BA tended to be increased in the  
630 HFD-GPE ( $p = 0.04$  versus HFD, Mann-Whitney test)(Fig 8F), whereas  
631 unconjugated BAs tended to be decreased ( $p = 0.04$ ) (Fig 8G). Similar to the  
632 cecum, no specific BA changed in concentration in the plasma (Fig 8H).

633 Bile acids are synthesized via the classical pathway under control of cholesterol  
634 7 alpha-hydroxylase (CYP7a1) and cholesterol 8 alpha-hydroxylase (CYP8a1), or  
635 via alternate pathways, such as the one under control of cholesterol 27-  
636 hydroxylase (CYP27a1) and cholesterol 7 beta-hydroxylase (CYP7b1). To  
637 determine whether our extracts could affect bile acid production, we measured  
638 the mRNA levels of the main factors controlling these pathways in the liver (Fig 9  
639 A-F) and ileum (Fig 9 G-H). We found a clear upregulation of CYP7a1 (Fig 9A)  
640 and a modest increase of CYP27a1 (Fig 9D) for the HFD-GPE mice, suggesting an  
641 increase in bile acid production in this group.

642 In the liver, bile acids can activate FXR, which has been shown to activate the  
643 expression of FGF15 in the intestine (55). FGF15 functions as a metabolic  
644 hormone, but also signals through FGFR4 in hepatocytes to inhibit expression of  
645 CYP7a1 gene, thereby acting as a negative feedback loop. Interestingly FGF15  
646 was upregulated in ileum of the HFD and HFD-GPE groups, but not in the HFD-  
647 CBE group (Fig 9H). Suggesting an enlarged bile acid pool in these mice. Why this  
648 is not reflected in the bile acid content remains to be determined.

## 649 Discussion

---

650 Although polyphenols are not strictly required for vital body functions in  
651 humans, there is compelling clinical and epidemiological evidence that they  
652 significantly reduce the risk of chronic diseases and promote health (7, 56, 57).  
653 However, a significant proportion of the population is not consuming sufficient  
654 quantities of dietary polyphenols as a result of inadequate vegetable and fruit  
655 intake. Therefore, concentrated polyphenol extracts might be valuable dietary  
656 supplements offering an interesting additional strategy for metabolic disorders  
657 management (12, 58, 59).

658 In this study, we demonstrated that both cinnamon bark and grape pomace  
659 extracts are able to ameliorate the overall metabolic profile in a model of diet-  
660 induced obesity. This is evidenced by a decrease in fat mass gain and adipose  
661 tissue inflammation and by reduced hepatic lipid content, especially in the grape  
662 pomace-treated mice, which was not compensated by elevated plasma lipid  
663 concentrations. Our data are consistent with previous reports that showed  
664 moderate but significant beneficial effect of table grape extracts on adiposity,  
665 hepatic steatosis, insulin resistance and adipose tissue inflammation (28, 30, 60-  
666 63).

667 We also found a clear improvement of glucose homeostasis by both extracts, as  
668 evidenced by an improved glucose tolerance and lower insulin resistance index.  
669 This was associated with a marked reduction of non-esterified fatty acids  
670 (NEFAs, free fatty acids), which have previously been found to be modulators of  
671 insulin sensitivity (64). Interestingly, although improvement of insulin resistance  
672 index was achieved by both grape and cinnamon extracts, the mechanisms

673 behind this seem to be different. Indeed, the HFD-GPE mice needed less insulin  
674 to achieve the same overall glucose profile, while the HFD-CBE mice had similar  
675 insulin secretion as HFD treated mice, but achieved faster glucose uptake. It has  
676 been proposed that cinnamon facilitates glucose entrance into cells by inducing  
677 glucose transporter 4 (GLUT4) translocation to the plasma membrane mediated  
678 by the LKB1-AMPK signalling pathway (65, 66), whereas grapes might activate  
679 the PI3K pathway and promote insulin action by reducing serine kinase  
680 activation and cytokine signaling (67). Our data thus suggest that both extracts  
681 might be useful additives in the management of glucose homeostasis in diabetic  
682 patients, as has been proposed previously (21, 23-25, 27).

683 A large fraction of dietary polyphenols reaches the colon and can be metabolized  
684 by the intestinal microbiota. Moreover, polyphenols are well known to affect  
685 intestinal bacteria (10, 11). Here, we report a significant impact of our extracts  
686 on the microbial composition, which was more profound for the GPE than for the  
687 CBE. One of the genera significantly increased by the GPE is *Roseburia*. These are  
688 bacteria that were previously found to be at a low abundance in patients with  
689 type 2 diabetes and proposed to play an important role in gut health as they have  
690 anti-inflammatory effects in the gut (68-70). Interestingly, *Roseburia* are  
691 increased by prebiotics and associated with improvements in metabolic  
692 disorders (71, 72). We also found a higher abundance of *Allobaculum*  
693 (*Erysipelotrichaceae*). This genus has also been shown to be increased by  
694 prebiotics (73, 74) and grape extracts (28), and has been associated with  
695 improved intestinal integrity, increased Reg3 $\gamma$  levels in the colon and with  
696 resistance to NAFLD development (50). Moreover, Metformin and Berberine,  
697 two clinically effective drugs for the treatment of diabetes, are associated with

698 increases in *Allobaculum* abundance (75). As for *Roseburia*, the major end  
699 product of *Allobaculum* fermentation is butyrate. This SCFA is of particular  
700 relevance in the gut because it is rapidly taken up by enterocytes where it serves  
701 as energy source (76). Conflicting data exist about the modulation of SCFA by  
702 polyphenols. Some studies reported an increase in SCFA after supplementation  
703 of the diet with extracts or phenolic compounds, whereas other studies showed  
704 no differences (77), but cecal SCFA content was not affected by treatments in our  
705 study (Fig 10A, B, D). GPE contains about 420 mg/g of fibers, which could be  
706 insufficient to induce a significant change in the microbial fermentation to  
707 markedly affect SCFA production. Alternatively, utilization of short-chain fatty  
708 acids by the colonocytes may be more important in this group. This is supported  
709 by the drastic increase of SLC5a8, a butyrate transporter, in the colon (Fig 10C).

710 As previously described, HFD feeding increased the abundance of  
711 Desulfovibrionaceae (73, 78) and *Lactococcus* (79). This was completely  
712 reversed with GPE. Several genera belonging to the Desulfovibrionaceae family  
713 are considered opportunistic pathogens and have been linked to some  
714 inflammatory diseases (80, 81). They produce endotoxins and have the capacity  
715 to reduce sulphate to H<sub>2</sub>S (82), thereby damaging the intestinal barrier (83).  
716 Indeed, H<sub>2</sub>S has been shown to disrupt energy metabolism in the gut epithelium  
717 (84). This leads to cell death and ultimately results in intestinal inflammation  
718 (85). As for the HFD-CBE mice, we found similar trends for *Roseburia*,  
719 *Desulfovibrio* and *Lactococcus* genera as in the HFD-GPE mice, although they did  
720 not reach statistical significance. While the genus *Peptococcus* was not  
721 consistently increased by HFD, we observed that CBE strongly decreased its  
722 level.

723 Previous studies have shown a strong association between the ingestion of  
724 polyphenol extracts and the species *Akkermansia muciniphila*, a bacterium  
725 known to improve metabolic disorders (12, 58). However, none of the tested  
726 treatments were associated with a modulation of *A. muciniphila* (data not  
727 shown). This was unexpected, as previous studies have shown an increase in  
728 abundance of *A. muciniphila* following polyphenol treatment (reviewed in (58)).  
729 In contrast, a recent study using a grape seed extract showed no changes in *A.*  
730 *muciniphila* (86) and it was also reported that Resveratrol, a polyphenol mainly  
731 found in grapes, berries and a wide range of fruits, decreases *A. muciniphila* in  
732 mice (87). In vitro, a pomegranate extract significantly inhibited the growth of *A.*  
733 *muciniphila* (88). This may suggest that polyphenols have varied prebiotic  
734 potential on *A. muciniphila*. However, there are several design differences  
735 between the studies that may have contributed to the divergent results  
736 concerning the gut microbiota composition. First, depending on the origin of the  
737 polyphenols (for example the grape terroir) and the extraction procedure the  
738 composition of the final extracts may vary significantly. Secondly, it has been  
739 shown that gut microbiota composition is affected by diet (type and amount of  
740 fat/sugar in the diet), mouse strain and age, and mouse provider (89). Thirdly,  
741 the increase of a certain bacterial species, such as *A. muciniphila*, may depend on  
742 its baseline intestinal abundance.

743 In accordance with our previous findings and the changes in the gut  
744 microbiota composition, the expression of several antimicrobial peptides,  
745 including Ang4 (effective against Gram-positive and Gram-negative bacteria),  
746 Reg3 $\gamma$  (effective against Gram-positive bacteria), and Lyz1 (mostly effective  
747 against Gram-positive bacteria) was found to be increased in response to both



748 CBE and GPE supplementation (90). In the CBE-treated group, this was  
749 accompanied by a putative increase in intestinal mucosal turnover and barrier  
750 integrity in the colon, as evidenced by an increase of intectin and claudin3.  
751 Gut microbiota may affect metabolic parameters by influencing the bile acid pool  
752 composition. Bile acids facilitate the digestion and absorption of lipids, but they  
753 also act as signaling molecules by binding to FXR, contributing to the regulation  
754 of various metabolic processes (91). Bile acid content tended to be increased  
755 with CBE, solely due to an increase in conjugated bile acids, suggesting a  
756 decrease in bile salt hydrolase (BSH) activity within the microbial community.  
757 This seems to be supported by the fact that we did not find any effect on the  
758 biological markers associated with the synthesis of bile acids in this group. In  
759 addition, evidence has revealed that bile acids are also able to alter the gut  
760 microbiota via direct and indirect antimicrobial effects (92), and promote the  
761 survival of some bile acid-tolerant bacteria such as  
762 some *Lactobacillus* and *Bifidobacterium* species (93). In contrast, we found  
763 evidence for an increase bile acid production in GPE treated mice. However, this  
764 was not translated to higher bile acid contents in caecum of plasma.  
765 Taken together, our data demonstrate that polyphenols derived from grapes or  
766 cinnamon can partially counter the deleterious effects of HFD and ameliorate  
767 overall metabolic parameters related to adiposity, glucose homeostasis and gut  
768 barrier integrity. These changes are associated with a modulation of the  
769 microbiota composition and a reduction in inflammation. Interestingly, all these  
770 beneficial effects resemble that of prebiotics, even though the doses used were  
771 much lower than those generally required for classical prebiotics (59, 94).

772 Modes of action of both compounds were found to be different, indicating that  
773 polyphenols have a broad range of targets that require further investigations.  
774 Thus, although both studied extracts positively improve glucose and lipid  
775 metabolism and reinforce the gut barrier together with changes in the gut  
776 microbiota, it is currently unknown how this beneficial effects occur. The health  
777 benefits on the host may be mediated by the microbial production of bioactive  
778 polyphenol-derived metabolites and/or by the modulation of the gut microbial  
779 community itself. Phenolic analysis indicated that the most abundant  
780 anthocyanins found in our grape pomace extract were Malvidin-3-O-glucoside,  
781 and Peonidin-3-O-glucoside (Table 2). While the antibesity and antidiabetic  
782 effects of anthocyanins have been demonstrated previously (29), the  
783 mechanisms by which these effects occur are still not clear and conflicting data  
784 still remain. Whether the beneficial effects can be attributed to a specific  
785 phenolic component or a single bacteria remains to be determined.  
786 Importantly, this study is the first reporting a change in animal gut microbes  
787 following treatment with a cinnamon extract, as well as a comprehensive  
788 phenotyping

789 In conclusion, our data as well as other reports strongly support the  
790 interest to use plant extracts rich in polyphenols to improve metabolic disorders  
791 associated with obesity and metabolic disorders.

## 792 Grants and funding

---

793 PDC is a research associate at FRS-FNRS (Fonds de la Recherche Scientifique),  
794 Belgium. HP and AE are research fellows at FRS-FNRS, Belgium. PDC is the  
795 recipient of grants from the FNRS, ERC Starting Grant 2013 (European Research  
796 Council, Starting grant 336452-ENIGMO), FRFS-WELBIO under grant: WELBIO-  
797 CR-2012S-02R and the Funds Baillet-Latour grant for medical research 2015.  
798 CD's researcher position is supported by a FIRST Spin-Off grant from the  
799 Walloon Region (convention 1410053).

800

## 801 Acknowledgments

---

802 We would like to thank A. Barrois, H. Danthinne, T. Pringels, M. Monnoye, C.  
803 Philippe and S. Boudebouze for excellent technical assistance. We thank R-M.  
804 Goebbels for the processing of the samples prior to histological analysis. We  
805 thank E. Bourny from the Laboratoire Provençal des Plantes Aromatiques  
806 (LPPAM), Buis les Baronnies, France, for the analysis of cinnamon extract.

807

## 808 Conflict of interests

---

809 PileJe (Saint-Laurent-des-Autels, France) provided funding for this study to PDC,  
810 PG and EM. AB, AG are employed by PiLeJe. There are no patents or products in  
811 development to declare.

- 813 1. <http://www.who.int/mediacentre/factsheets/fs311/en/>.
- 814 2. **Bogardus C.** Missing heritability and GWAS utility. *Obesity (Silver Spring)*  
815 17: 209-210, 2009.
- 816 3. **Pi-Sunyer X.** The medical risks of obesity. *Postgrad Med* 121: 21-33,  
817 2009.
- 818 4. **Christian JG, Tsai AG, and Bessesen DH.** Interpreting weight losses from  
819 lifestyle modification trials: using categorical data. *Int J Obes (Lond)* 34: 207-209,  
820 2010.
- 821 5. **Patel D.** Pharmacotherapy for the management of obesity. *Metabolism* 64:  
822 1376-1385, 2015.
- 823 6. **Thaiss CA, Itav S, Rothschild D, Meijer M, Levy M, Moresi C,**  
824 **Dohnalova L, Braverman S, Rozin S, Malitsky S, Dori-Bachash M, Kuperman**  
825 **Y, Biton I, Gertler A, Harmelin A, Shapiro H, Halpern Z, Aharoni A, Segal E,**  
826 **and Elinav E.** Persistent microbiome alterations modulate the rate of post-  
827 dieting weight regain. *Nature* 2016.
- 828 7. **Del Rio D, Rodriguez-Mateos A, Spencer JP, Tognolini M, Borges G,**  
829 **and Crozier A.** Dietary (poly)phenolics in human health: structures,  
830 bioavailability, and evidence of protective effects against chronic diseases.  
831 *Antioxid Redox Signal* 18: 1818-1892, 2013.
- 832 8. **Chuang CC, and McIntosh MK.** Potential mechanisms by which  
833 polyphenol-rich grapes prevent obesity-mediated inflammation and metabolic  
834 diseases. *Annu Rev Nutr* 31: 155-176, 2011.
- 835 9. **Selma MV, Espin JC, and Tomas-Barberan FA.** Interaction between  
836 phenolics and gut microbiota: role in human health. *J Agric Food Chem* 57: 6485-  
837 6501, 2009.
- 838 10. **Nohynek LJ, Alakomi HL, Kahkonen MP, Heinonen M, Helander IM,**  
839 **Oksman-Caldentey KM, and Puupponen-Pimia RH.** Berry phenolics:  
840 antimicrobial properties and mechanisms of action against severe human  
841 pathogens. *Nutr Cancer* 54: 18-32, 2006.
- 842 11. **Puupponen-Pimia R, Nohynek L, Meier C, Kahkonen M, Heinonen M,**  
843 **Hopia A, and Oksman-Caldentey KM.** Antimicrobial properties of phenolic  
844 compounds from berries. *J Appl Microbiol* 90: 494-507, 2001.
- 845 12. **Anhe FF, Roy D, Pilon G, Dudonne S, Matamoros S, Varin TV, Garofalo**  
846 **C, Moine Q, Desjardins Y, Levy E, and Marette A.** A polyphenol-rich cranberry  
847 extract protects from diet-induced obesity, insulin resistance and intestinal  
848 inflammation in association with increased Akkermansia spp. population in the  
849 gut microbiota of mice. *Gut* 64: 872-883, 2015.
- 850 13. **Cani PD, Dewever C, and Delzenne NM.** Inulin-type fructans modulate  
851 gastrointestinal peptides involved in appetite regulation (glucagon-like peptide-  
852 1 and ghrelin) in rats. *Br J Nutr* 92: 521-526, 2004.
- 853 14. **Backhed F, Ding H, Wang T, Hooper LV, Koh GY, Nagy A, Semenkovich**  
854 **CF, and Gordon JI.** The gut microbiota as an environmental factor that regulates  
855 fat storage. *Proc Natl Acad Sci U S A* 101: 15718-15723, 2004.
- 856 15. **Turnbaugh PJ, Ley RE, Mahowald MA, Magrini V, Mardis ER, and**  
857 **Gordon JI.** An obesity-associated gut microbiome with increased capacity for  
858 energy harvest. *Nature* 444: 1027-1031, 2006.

- 859 16. **Rabot S, Membrez M, Bruneau A, Gerard P, Harach T, Moser M,**  
860 **Raymond F, Mansourian R, and Chou CJ.** Germ-free C57BL/6J mice are  
861 resistant to high-fat-diet-induced insulin resistance and have altered cholesterol  
862 metabolism. *FASEB J* 24: 4948-4959, 2010.
- 863 17. **Cani PD, Amar J, Iglesias MA, Poggi M, Knauf C, Bastelica D, Neyrinck**  
864 **AM, Fava F, Tuohy KM, Chabo C, Waget A, Delmee E, Cousin B, Sulpice T,**  
865 **Chamontin B, Ferrieres J, Tanti JF, Gibson GR, Casteilla L, Delzenne NM,**  
866 **Alessi MC, and Burcelin R.** Metabolic endotoxemia initiates obesity and insulin  
867 resistance. *Diabetes* 56: 1761-1772, 2007.
- 868 18. **Cani PD, Bibiloni R, Knauf C, Waget A, Neyrinck AM, Delzenne NM,**  
869 **and Burcelin R.** Changes in gut microbiota control metabolic endotoxemia-  
870 induced inflammation in high-fat diet-induced obesity and diabetes in mice.  
871 *Diabetes* 57: 1470-1481, 2008.
- 872 19. **Cani PD.** Metabolism in 2013: The gut microbiota manages host  
873 metabolism. *Nat Rev Endocrinol* 10: 74-76, 2014.
- 874 20. **Cani PD, and Everard A.** Talking microbes: When gut bacteria interact  
875 with diet and host organs. *Mol Nutr Food Res* 60: 58-66, 2016.
- 876 21. **Liu Y, Cotillard A, Vazier C, Bastard JP, Fellahi S, Stevant M, Allatif O,**  
877 **Langlois C, Bieuvelet S, Brochot A, Guilbot A, Clement K, and Rizkalla SW.** A  
878 Dietary Supplement Containing Cinnamon, Chromium and Carnosine Decreases  
879 Fasting Plasma Glucose and Increases Lean Mass in Overweight or Obese Pre-  
880 Diabetic Subjects: A Randomized, Placebo-Controlled Trial. *PLoS One* 10:  
881 e0138646, 2015.
- 882 22. **Qin B, Dawson H, Polansky MM, and Anderson RA.** Cinnamon extract  
883 attenuates TNF-alpha-induced intestinal lipoprotein ApoB48 overproduction by  
884 regulating inflammatory, insulin, and lipoprotein pathways in enterocytes. *Horm*  
885 *Metab Res* 41: 516-522, 2009.
- 886 23. **Qin B, Nagasaki M, Ren M, Bajotto G, Oshida Y, and Sato Y.** Cinnamon  
887 extract (traditional herb) potentiates in vivo insulin-regulated glucose utilization  
888 via enhancing insulin signaling in rats. *Diabetes Res Clin Pract* 62: 139-148, 2003.
- 889 24. **Qin B, Nagasaki M, Ren M, Bajotto G, Oshida Y, and Sato Y.** Cinnamon  
890 extract prevents the insulin resistance induced by a high-fructose diet. *Horm*  
891 *Metab Res* 36: 119-125, 2004.
- 892 25. **Ziegenfuss TN, Hofheins JE, Mendel RW, Landis J, and Anderson RA.**  
893 Effects of a water-soluble cinnamon extract on body composition and features of  
894 the metabolic syndrome in pre-diabetic men and women. *J Int Soc Sports Nutr* 3:  
895 45-53, 2006.
- 896 26. **Ranasinghe P, Jayawardana R, Galappaththy P, Constantine GR, de**  
897 **Vas Gunawardana N, and Katulanda P.** Efficacy and safety of 'true' cinnamon  
898 (*Cinnamomum zeylanicum*) as a pharmaceutical agent in diabetes: a systematic  
899 review and meta-analysis. *Diabet Med* 29: 1480-1492, 2012.
- 900 27. **Akaberi M, and Hosseinzadeh H.** Grapes (*Vitis vinifera*) as a Potential  
901 Candidate for the Therapy of the Metabolic Syndrome. *Phytother Res* 30: 540-  
902 556, 2016.
- 903 28. **Collins B, Hoffman J, Martinez K, Grace M, Lila MA, Cockrell C,**  
904 **Nadimpalli A, Chang E, Chuang CC, Zhong W, Mackert J, Shen W, Cooney P,**  
905 **Hopkins R, and McIntosh M.** A polyphenol-rich fraction obtained from table  
906 grapes decreases adiposity, insulin resistance and markers of inflammation and  
907 impacts gut microbiota in high-fat-fed mice. *J Nutr Biochem* 31: 150-165, 2016.

- 908 29. **He J, and Giusti MM.** Anthocyanins: natural colorants with health-  
 909 promoting properties. *Annu Rev Food Sci Technol* 1: 163-187, 2010.
- 910 30. **Baldwin J, Collins B, Wolf PG, Martinez K, Shen W, Chuang CC, Zhong**  
 911 **W, Cooney P, Cockrell C, Chang E, Gaskins HR, and McIntosh MK.** Table grape  
 912 consumption reduces adiposity and markers of hepatic lipogenesis and alters gut  
 913 microbiota in butter fat-fed mice. *J Nutr Biochem* 27: 123-135, 2016.
- 914 31. **Roopchand DE, Carmody RN, Kuhn P, Moskal K, Rojas-Silva P,**  
 915 **Turnbaugh PJ, and Raskin I.** Dietary Polyphenols Promote Growth of the Gut  
 916 Bacterium *Akkermansia muciniphila* and Attenuate High-Fat Diet-Induced  
 917 Metabolic Syndrome. *Diabetes* 64: 2847-2858, 2015.
- 918 32. **Wang H, Xue Y, Zhang H, Huang Y, Yang G, Du M, and Zhu MJ.** Dietary  
 919 grape seed extract ameliorates symptoms of inflammatory bowel disease in  
 920 IL10-deficient mice. *Mol Nutr Food Res* 57: 2253-2257, 2013.
- 921 33. **Anderson RA, Broadhurst CL, Polansky MM, Schmidt WF, Khan A,**  
 922 **Flanagan VP, Schoene NW, and Graves DJ.** Isolation and characterization of  
 923 polyphenol type-A polymers from cinnamon with insulin-like biological activity. *J*  
 924 *Agric Food Chem* 52: 65-70, 2004.
- 925 34. **Kammerer D, Claus A, Carle R, and Schieber A.** Polyphenol screening of  
 926 pomace from red and white grape varieties (*Vitis vinifera* L.) by HPLC-DAD-  
 927 MS/MS. *J Agric Food Chem* 52: 4360-4367, 2004.
- 928 35. **Cani PD, Amar J, Iglesias MA, Poggi M, Knauf C, Bastelica D, Neyrinck**  
 929 **AM, Fava F, Tuohy KM, Chabo C, Waget A, Delmee E, Cousin B, Sulpice T,**  
 930 **Chamontin B, Ferrieres J, Tanti JF, Gibson GR, Casteilla L, Delzenne NM,**  
 931 **Alessi MC, and Burcelin R.** Metabolic endotoxemia initiates obesity and insulin  
 932 resistance. *Diabetes* 56: 1761-1772, 2007.
- 933 36. **Geurts L, Everard A, Van Hul M, Essaghir A, Duparc T, Matamoros S,**  
 934 **Plovier H, Castel J, Denis RG, Bergiers M, Druart C, Alhouayek M, Delzenne**  
 935 **NM, Muccioli GG, Demoulin JB, Luquet S, and Cani PD.** Adipose tissue NAPE-  
 936 PLD controls fat mass development by altering the browning process and gut  
 937 microbiota. *Nat Commun* 6: 6495, 2015.
- 938 37. **Everard A, Geurts L, Caesar R, Van Hul M, Matamoros S, Duparc T,**  
 939 **Denis RG, Cochez P, Pierard F, Castel J, Bindels LB, Plovier H, Robine S,**  
 940 **Muccioli GG, Renauld JC, Dumoutier L, Delzenne NM, Luquet S, Backhed F,**  
 941 **and Cani PD.** Intestinal epithelial MyD88 is a sensor switching host metabolism  
 942 towards obesity according to nutritional status. *Nat Commun* 5: 5648, 2014.
- 943 38. **Folch J, Lees M, and Sloane Stanley GH.** A simple method for the  
 944 isolation and purification of total lipides from animal tissues. *J Biol Chem* 226:  
 945 497-509, 1957.
- 946 39. **Lan A, Bruneau A, Bensaada M, Philippe C, Bellaud P, Rabot S, and Jan**  
 947 **G.** Increased induction of apoptosis by *Propionibacterium freudenreichii* TL133  
 948 in colonic mucosal crypts of human microbiota-associated rats treated with 1,2-  
 949 dimethylhydrazine. *Br J Nutr* 100: 1251-1259, 2008.
- 950 40. **Tremaroli V, Karlsson F, Werling M, Stahlman M, Kovatcheva-**  
 951 **Datchary P, Olbers T, Fandriks L, le Roux CW, Nielsen J, and Backhed F.**  
 952 Roux-en-Y Gastric Bypass and Vertical Banded Gastroplasty Induce Long-Term  
 953 Changes on the Human Gut Microbiome Contributing to Fat Mass Regulation. *Cell*  
 954 *Metab* 22: 228-238, 2015.
- 955 41. **Magoc T, and Salzberg SL.** FLASH: fast length adjustment of short reads  
 956 to improve genome assemblies. *Bioinformatics* 27: 2957-2963, 2011.

- 957 42. **Schloss PD, Westcott SL, Ryabin T, Hall JR, Hartmann M, Hollister EB,**  
958 **Lesniewski RA, Oakley BB, Parks DH, Robinson CJ, Sahl JW, Stres B,**  
959 **Thallinger GG, Van Horn DJ, and Weber CF.** Introducing mothur: open-source,  
960 platform-independent, community-supported software for describing and  
961 comparing microbial communities. *Appl Environ Microbiol* 75: 7537-7541, 2009.
- 962 43. **Edgar RC, Haas BJ, Clemente JC, Quince C, and Knight R.** UCHIME  
963 improves sensitivity and speed of chimera detection. *Bioinformatics* 27: 2194-  
964 2200, 2011.
- 965 44. **Sun Y, Cai Y, Huse SM, Knight R, Farmerie WG, Wang X, and Mai V.** A  
966 large-scale benchmark study of existing algorithms for taxonomy-independent  
967 microbial community analysis. *Brief Bioinform* 13: 107-121, 2011.
- 968 45. **DeSantis TZ, Hugenholtz P, Larsen N, Rojas M, Brodie EL, Keller K,**  
969 **Huber T, Dalevi D, Hu P, and Andersen GL.** Greengenes, a chimera-checked  
970 16S rRNA gene database and workbench compatible with ARB. *Appl Environ*  
971 *Microbiol* 72: 5069-5072, 2006.
- 972 46. **Wang Q, Garrity GM, Tiedje JM, and Cole JR.** Naive Bayesian classifier  
973 for rapid assignment of rRNA sequences into the new bacterial taxonomy. *Appl*  
974 *Environ Microbiol* 73: 5261-5267, 2007.
- 975 47. **Hochberg Y, and Benjamini Y.** More powerful procedures for multiple  
976 significance testing. *Stat Med* 9: 811-818, 1990.
- 977 48. **Kanda H, Tateya S, Tamori Y, Kotani K, Hiasa K, Kitazawa R, Kitazawa**  
978 **S, Miyachi H, Maeda S, Egashira K, and Kasuga M.** MCP-1 contributes to  
979 macrophage infiltration into adipose tissue, insulin resistance, and hepatic  
980 steatosis in obesity. *J Clin Invest* 116: 1494-1505, 2006.
- 981 49. **Patsouris D, Li PP, Thapar D, Chapman J, Olefsky JM, and Neels JG.**  
982 Ablation of CD11c-positive cells normalizes insulin sensitivity in obese insulin  
983 resistant animals. *Cell Metab* 8: 301-309, 2008.
- 984 50. **Le Roy T, Llopis M, Lepage P, Bruneau A, Rabot S, Bevilacqua C,**  
985 **Martin P, Philippe C, Walker F, Bado A, Perlemuter G, Cassard-Doulier AM,**  
986 **and Gerard P.** Intestinal microbiota determines development of non-alcoholic  
987 fatty liver disease in mice. *Gut* 62: 1787-1794, 2013.
- 988 51. **Backhed F, Manchester JK, Semenkovich CF, and Gordon JI.**  
989 Mechanisms underlying the resistance to diet-induced obesity in germ-free mice.  
990 *Proc Natl Acad Sci U S A* 104: 979-984, 2007.
- 991 52. **Cani PD, Possemiers S, Van de Wiele T, Guiot Y, Everard A, Rottier O,**  
992 **Geurts L, Naslain D, Neyrinck A, Lambert DM, Muccioli GG, and Delzenne**  
993 **NM.** Changes in gut microbiota control inflammation in obese mice through a  
994 mechanism involving GLP-2-driven improvement of gut permeability. *Gut* 58:  
995 1091-1103, 2009.
- 996 53. **Gerard P.** Metabolism of cholesterol and bile acids by the gut microbiota.  
997 *Pathogens* 3: 14-24, 2013.
- 998 54. **Sayin SI, Wahlstrom A, Felin J, Jantti S, Marschall HU, Bamberg K,**  
999 **Angelin B, Hyotylainen T, Oresic M, and Backhed F.** Gut microbiota regulates  
1000 bile acid metabolism by reducing the levels of tauro-beta-muricholic acid, a  
1001 naturally occurring FXR antagonist. *Cell Metab* 17: 225-235, 2013.
- 1002 55. **Inagaki T, Choi M, Moschetta A, Peng L, Cummins CL, McDonald JG,**  
1003 **Luo G, Jones SA, Goodwin B, Richardson JA, Gerard RD, Repa JJ, Mangelsdorf**  
1004 **DJ, and Kliewer SA.** Fibroblast growth factor 15 functions as an enterohepatic  
1005 signal to regulate bile acid homeostasis. *Cell Metab* 2: 217-225, 2005.

- 1006 56. **Blade C, Aragonés G, Arola-Arnal A, Muguerza B, Bravo FI, Salvado**  
1007 **MJ, Arola L, and Suarez M.** Proanthocyanidins in health and disease. *Biofactors*  
1008 42: 5-12, 2016.
- 1009 57. **Zhang PY.** Polyphenols in Health and Disease. *Cell Biochem Biophys* 73:  
1010 649-664, 2015.
- 1011 58. **Anhe FF, Pilon G, Roy D, Desjardins Y, Levy E, and Marette A.**  
1012 Triggering Akkermansia with dietary polyphenols: A new weapon to combat the  
1013 metabolic syndrome? *Gut Microbes* 7: 146-153, 2016.
- 1014 59. **Anhe FF, Varin TV, Le Barz M, Desjardins Y, Levy E, Roy D, and**  
1015 **Marette A.** Gut Microbiota Dysbiosis in Obesity-Linked Metabolic Diseases and  
1016 Prebiotic Potential of Polyphenol-Rich Extracts. *Curr Obes Rep* 4: 389-400, 2015.
- 1017 60. **Suwannaphet W, Meeprom A, Yibchok-Anun S, and Adisakwattana S.**  
1018 Preventive effect of grape seed extract against high-fructose diet-induced insulin  
1019 resistance and oxidative stress in rats. *Food Chem Toxicol* 48: 1853-1857, 2010.
- 1020 61. **Park SH, Park TS, and Cha YS.** Grape seed extract (*Vitis vinifera*)  
1021 partially reverses high fat diet-induced obesity in C57BL/6J mice. *Nutr Res Pract*  
1022 2: 227-233, 2008.
- 1023 62. **Terra X, Pallares V, Ardevol A, Blade C, Fernandez-Larrea J, Pujadas**  
1024 **G, Salvado J, Arola L, and Blay M.** Modulatory effect of grape-seed procyanidins  
1025 on local and systemic inflammation in diet-induced obesity rats. *J Nutr Biochem*  
1026 22: 380-387, 2011.
- 1027 63. **Gourineni V, Shay NF, Chung S, Sandhu AK, and Gu L.** Muscadine grape  
1028 (*Vitis rotundifolia*) and wine phytochemicals prevented obesity-associated  
1029 metabolic complications in C57BL/6J mice. *J Agric Food Chem* 60: 7674-7681,  
1030 2012.
- 1031 64. **Kahn SE, Hull RL, and Utzschneider KM.** Mechanisms linking obesity to  
1032 insulin resistance and type 2 diabetes. *Nature* 444: 840-846, 2006.
- 1033 65. **Absalan A, Mohiti-Ardakani J, Hadinedoushan H, and Khalili MA.**  
1034 Hydro-Alcoholic Cinnamon Extract, Enhances Glucose Transporter Isotype-4  
1035 Translocation from Intracellular Compartments into the Cytoplasmic Membrane  
1036 of C2C12 Myotubes. *Indian J Clin Biochem* 27: 351-356, 2012.
- 1037 66. **Shen Y, Honma N, Kobayashi K, Jia LN, Hosono T, Shindo K, Ariga T,**  
1038 **and Seki T.** Cinnamon extract enhances glucose uptake in 3T3-L1 adipocytes  
1039 and C2C12 myocytes by inducing LKB1-AMP-activated protein kinase signaling.  
1040 *PLoS One* 9: e87894, 2014.
- 1041 67. **Yogalakshmi B, Bhuvaneshwari S, Sreeja S, and Anuradha CV.** Grape  
1042 seed proanthocyanidins and metformin act by different mechanisms to promote  
1043 insulin signaling in rats fed high calorie diet. *J Cell Commun Signal* 8: 13-22, 2014.
- 1044 68. **Aminov RI, Walker AW, Duncan SH, Harmsen HJ, Welling GW, and**  
1045 **Flint HJ.** Molecular diversity, cultivation, and improved detection by fluorescent  
1046 in situ hybridization of a dominant group of human gut bacteria related to  
1047 *Roseburia* spp. or *Eubacterium rectale*. *Appl Environ Microbiol* 72: 6371-6376,  
1048 2006.
- 1049 69. **Karlsson FH, Tremaroli V, Nookaew I, Bergstrom G, Behre CJ,**  
1050 **Fagerberg B, Nielsen J, and Backhed F.** Gut metagenome in European women  
1051 with normal, impaired and diabetic glucose control. *Nature* 498: 99-103, 2013.
- 1052 70. **Qin J, Li Y, Cai Z, Li S, Zhu J, Zhang F, Liang S, Zhang W, Guan Y, Shen D,**  
1053 **Peng Y, Zhang D, Jie Z, Wu W, Qin Y, Xue W, Li J, Han L, Lu D, Wu P, Dai Y, Sun**  
1054 **X, Li Z, Tang A, Zhong S, Li X, Chen W, Xu R, Wang M, Feng Q, Gong M, Yu J,**



- 1055 **Zhang Y, Zhang M, Hansen T, Sanchez G, Raes J, Falony G, Okuda S, Almeida**  
 1056 **M, LeChatelier E, Renault P, Pons N, Batto JM, Zhang Z, Chen H, Yang R,**  
 1057 **Zheng W, Li S, Yang H, Wang J, Ehrlich SD, Nielsen R, Pedersen O,**  
 1058 **Kristiansen K, and Wang J.** A metagenome-wide association study of gut  
 1059 microbiota in type 2 diabetes. *Nature* 490: 55-60, 2012.
- 1060 71. **Neyrinck AM, Possemiers S, Druart C, Van de Wiele T, De Backer F,**  
 1061 **Cani PD, Larondelle Y, and Delzenne NM.** Prebiotic effects of wheat  
 1062 arabinoxylan related to the increase in bifidobacteria, Roseburia and  
 1063 Bacteroides/Prevotella in diet-induced obese mice. *PLoS One* 6: e20944, 2011.
- 1064 72. **Neyrinck AM, Possemiers S, Verstraete W, De Backer F, Cani PD, and**  
 1065 **Delzenne NM.** Dietary modulation of clostridial cluster XIVa gut bacteria  
 1066 (Roseburia spp.) by chitin-glucan fiber improves host metabolic alterations  
 1067 induced by high-fat diet in mice. *J Nutr Biochem* 23: 51-59, 2012.
- 1068 73. **Everard A, Lazarevic V, Gaia N, Johansson M, Stahlman M, Backhed F,**  
 1069 **Delzenne NM, Schrenzel J, Francois P, and Cani PD.** Microbiome of prebiotic-  
 1070 treated mice reveals novel targets involved in host response during obesity.  
 1071 *ISME J* 8: 2116-2130, 2014.
- 1072 74. **Tachon S, Zhou J, Keenan M, Martin R, and Marco ML.** The intestinal  
 1073 microbiota in aged mice is modulated by dietary resistant starch and correlated  
 1074 with improvements in host responses. *FEMS Microbiol Ecol* 83: 299-309, 2013.
- 1075 75. **Zhang X, Zhao Y, Xu J, Xue Z, Zhang M, Pang X, Zhang X, and Zhao L.**  
 1076 Modulation of gut microbiota by berberine and metformin during the treatment  
 1077 of high-fat diet-induced obesity in rats. *Sci Rep* 5: 14405, 2015.
- 1078 76. **Donohoe DR, Garge N, Zhang X, Sun W, O'Connell TM, Bunker MK,**  
 1079 **and Bultman SJ.** The microbiome and butyrate regulate energy metabolism and  
 1080 autophagy in the mammalian colon. *Cell Metab* 13: 517-526, 2011.
- 1081 77. **Mosele JI, Macia A, and Motilva MJ.** Metabolic and Microbial Modulation  
 1082 of the Large Intestine Ecosystem by Non-Absorbed Diet Phenolic Compounds: A  
 1083 Review. *Molecules* 20: 17429-17468, 2015.
- 1084 78. **Zhang C, Zhang M, Pang X, Zhao Y, Wang L, and Zhao L.** Structural  
 1085 resilience of the gut microbiota in adult mice under high-fat dietary  
 1086 perturbations. *ISME J* 6: 1848-1857, 2012.
- 1087 79. **Parks BW, Nam E, Org E, Kostem E, Norheim F, Hui ST, Pan C, Civelek**  
 1088 **M, Rau CD, Bennett BJ, Mehrabian M, Ursell LK, He A, Castellani LW, Zinker**  
 1089 **B, Kirby M, Drake TA, Drevon CA, Knight R, Gargalovic P, Kirchgessner T,**  
 1090 **Eskin E, and Lusic AJ.** Genetic control of obesity and gut microbiota composition  
 1091 in response to high-fat, high-sucrose diet in mice. *Cell Metab* 17: 141-152, 2013.
- 1092 80. **Loubinoux J, Mory F, Pereira IA, and Le Faou AE.** Bacteremia caused by  
 1093 a strain of *Desulfovibrio* related to the provisionally named *Desulfovibrio*  
 1094 *fairfieldensis*. *J Clin Microbiol* 38: 931-934, 2000.
- 1095 81. **Weglarz L, Dzierzewicz Z, Skop B, Orchel A, Parfiniewicz B,**  
 1096 **Wisniowska B, Swiatkowska L, and Wilczok T.** *Desulfovibrio desulfuricans*  
 1097 lipopolysaccharides induce endothelial cell IL-6 and IL-8 secretion and E-selectin  
 1098 and VCAM-1 expression. *Cell Mol Biol Lett* 8: 991-1003, 2003.
- 1099 82. **Wagner M, Roger AJ, Flax JL, Brusseau GA, and Stahl DA.** Phylogeny of  
 1100 dissimilatory sulfite reductases supports an early origin of sulfate respiration. *J*  
 1101 *Bacteriol* 180: 2975-2982, 1998.
- 1102 83. **Jakobsson HE, Rodriguez-Pineiro AM, Schutte A, Ermund A, Boysen P,**  
 1103 **Bemark M, Sommer F, Backhed F, Hansson GC, and Johansson ME.** The

- 1104 composition of the gut microbiota shapes the colon mucus barrier. *EMBO Rep* 16:  
1105 164-177, 2015.
- 1106 84. **Babidge W, Millard S, and Roediger W.** Sulfides impair short chain fatty  
1107 acid beta-oxidation at acyl-CoA dehydrogenase level in colonocytes: implications  
1108 for ulcerative colitis. *Mol Cell Biochem* 181: 117-124, 1998.
- 1109 85. **Den Hond E, Hiele M, Evenepoel P, Peeters M, Ghos Y, and Rutgeerts**  
1110 **P.** In vivo butyrate metabolism and colonic permeability in extensive ulcerative  
1111 colitis. *Gastroenterology* 115: 584-590, 1998.
- 1112 86. **Liu W, Zhao S, Wang J, Shi J, Sun Y, Wang W, Ning G, Hong J, and Liu R.**  
1113 Grape seed proanthocyanidin extract ameliorates inflammation and adiposity by  
1114 modulating gut microbiota in high-fat diet mice. *Mol Nutr Food Res* 2017.
- 1115 87. **Sung MM, Kim TT, Denou E, Soltys CM, Hamza SM, Byrne NJ, Masson**  
1116 **G, Park H, Wishart DS, Madsen KL, Schertzer JD, and Dyck JR.** Improved  
1117 Glucose Homeostasis in Obese Mice Treated With Resveratrol Is Associated With  
1118 Alterations in the Gut Microbiome. *Diabetes* 66: 418-425, 2017.
- 1119 88. **Henning SM, Summanen PH, Lee RP, Yang J, Finegold SM, Heber D,**  
1120 **and Li Z.** Pomegranate ellagitannins stimulate the growth of *Akkermansia*  
1121 *muciniphila* in vivo. *Anaerobe* 43: 56-60, 2017.
- 1122 89. **Laukens D, Brinkman BM, Raes J, De Vos M, and Vandenabeele P.**  
1123 Heterogeneity of the gut microbiome in mice: guidelines for optimizing  
1124 experimental design. *FEMS Microbiol Rev* 40: 117-132, 2016.
- 1125 90. **Gallo RL, and Hooper LV.** Epithelial antimicrobial defence of the skin and  
1126 intestine. *Nat Rev Immunol* 12: 503-516, 2012.
- 1127 91. **Wang YD, Chen WD, Moore DD, and Huang W.** FXR: a metabolic  
1128 regulator and cell protector. *Cell Res* 18: 1087-1095, 2008.
- 1129 92. **Begley M, Gahan CG, and Hill C.** The interaction between bacteria and  
1130 bile. *FEMS Microbiol Rev* 29: 625-651, 2005.
- 1131 93. **Devkota S, Wang Y, Musch MW, Leone V, Fehlner-Peach H,**  
1132 **Nadimpalli A, Antonopoulos DA, Jabri B, and Chang EB.** Dietary-fat-induced  
1133 taurocholic acid promotes pathobiont expansion and colitis in *Il10*<sup>-/-</sup> mice.  
1134 *Nature* 487: 104-108, 2012.
- 1135 94. **Bindels LB, Delzenne NM, Cani PD, and Walter J.** Towards a more  
1136 comprehensive concept for prebiotics. *Nat Rev Gastroenterol Hepatol* 12: 303-  
1137 310, 2015.
- 1138
- 1139

## 1140 Figure Legends

1141

### 1142 **Figure 1. Effects on body composition and adipose tissue.**

1143 8 week follow up of (A) body weight (g) with corresponding (B) fat mass (g) and  
1144 (C) lean mass (g) measured by TD-NMR. (D) Body weight gain (g), (E) fat mass  
1145 (g), (F) fat mass and lean mass (% of total body weight) at the end of the follow  
1146 up. (G) Weight of brown adipose tissue (mg). (H) Weights of subcutaneous,  
1147 epididymal and visceral adipose tissues (mg) and corresponding (I) adiposity  
1148 index (%white adipose tissue/body weight). (J) Leptin plasma levels (ng/ml).  
1149 Data are presented as the mean±s.e.m. ‘\*’ ‘\*\*’ and ‘#’ indicate a significant  
1150 difference versus HFD (P<0.05, P<0.01, P<0.001 respectively) as determined by a  
1151 two-way ANOVA (A-C). Data with different superscript letters are significantly  
1152 different (P<0.05) according to post-hoc one-way ANOVA (D-J).

1153

### 1154 **Figure 2. Effects on Glucose homeostasis.**

1155 (A) Plasma glucose (mg/dl) profile and (B) the mean area under the curve (AUC)  
1156 measured between 0 and 120 min after glucose loading (mg/dl/min). (C) Plasma  
1157 insulin levels at 30 min before and 15 min after glucose loading (µg/l). (D)  
1158 Glucose-induced insulin secretion, calculated as the difference between the  
1159 fasting insulinemia and the insulinemia 15 min after an oral glucose load. (E)  
1160 Insulin resistance index determined by multiplying the AUC of blood glucose by  
1161 the AUC of insulin between 30 min before and 15 min after glucose loading. (F)  
1162 Adipocyte distribution and frequency with respect to the mean diameter  
1163 measured by histological analysis. (G) Mean adipocyte size (µm). (H) Resistin  
1164 plasma levels measured in the vena cava (ng/ml). Data are presented as the  
1165 mean±s.e.m. ‘\*’ ‘\*\*’ and ‘#’ indicate a significant difference versus HFD (P<0.05,  
1166 P<0.01, P<0.001 respectively) as determined by a two-way ANOVA (A-B). Data  
1167 with different superscript letters are significantly different (P<0.05) according to  
1168 post-hoc one-way ANOVA (B-E).

1169

### 1170 **Figure 3. Effects on energy metabolism.**

1171 Energy intake: (A) mean food intake per week per mouse (kcal). Energy  
1172 excretion: (B) mean amount of feces excreted per mouse in 24h (mg/24h), (C)  
1173 mean energy content in feces (kcal/g) and (D) daily energy excretion as  
1174 calculated using the previous values (kcal/mouse) and (E) as percentage of the  
1175 food intake. (F) Energy expenditure per night per mouse (kcal/h/kg). (G) Daily  
1176 energy expenditure (kCal/h/kg), (H) body temperature (°C) and (I) respiratory  
1177 exchange ratio (RER). (J) Cumulative mean number of beam breaks recorded per  
1178 mouse during six days. (J) qPCR analysis of glucose transporters SGLT1 and  
1179 GLUT2, and of fatty acid transporters LFABP and CD36. Data are presented as the  
1180 mean±s.e.m. Data with different superscript letters are significantly different  
1181 (P<0.05) according to post-hoc one-way ANOVA (A-E). ‘\*’ and ‘\*\*’ indicate a

1182 significant difference versus HFD ( $P<0.05$  and  $P<0.01$  respectively) as  
1183 determined by a two-way ANOVA (F).

1184

1185 **Figure 4. Effects on lipid homeostasis.**

1186 (A) Plasmatic concentrations of non-esterified fatty acids (NEFAs) (mM),  
1187 cholesterol (mg/dl) and triglycerides (mg/dl). (B) Hepatic total lipid content  
1188 (mg/100mg tissue), cholesterol (mmol/mg tissue) and triglycerides (mmol/mg  
1189 tissue),

1190 (C) Representative Oil Red O pictures of the liver with quantitative measurement  
1191 (%). Data are presented as the mean $\pm$ s.e.m. Data with different superscript  
1192 letters are significantly different ( $P<0.05$ ) according to post-hoc one-way  
1193 ANOVA.

1194

1195 **Figure 5. Effects on adipose tissue inflammation.**

1196 qPCR analysis of macrophage markers mRNA expression (A) in the subcutaneous  
1197 and (B) the visceral adipose tissue (fold change versus CT group). (C)  
1198 Representative staining of MAC2 with Hematoxylin counterstaining of  
1199 subcutaneous adipose tissues and quantitative measurements of the mean  
1200 number of positive cells per adipocyte counted. (D) Plasma concentrations of  
1201 different inflammatory markers. Data are presented as the mean $\pm$ s.e.m. Data  
1202 with different superscript letters are significantly different ( $P<0.05$ ) according to  
1203 post-hoc one-way ANOVA.

1204

1205 **Figure 6. Effects on gut microbiota.**

1206 Gut bacterial community analysis by 16S rRNA gene high-throughput  
1207 sequencing. (A) Composition of abundant bacterial phyla identified in the  
1208 microbiota of the four different groups. (B) OTUs significantly affected by grape  
1209 or cinnamon supplementation under HFD. A representative 16S rRNA gene from  
1210 each of the differentially expressed OTUs versus HFD mice was aligned and used  
1211 to infer the phylogenetic trees shown in this figure. The color of the OTU  
1212 indicates its family. (C) Principal coordinate analysis based on the weighted  
1213 UniFrac analysis (PCoA + WUF) on operational taxonomic units (OTUs). Each  
1214 symbol representing a single sample is colored according to the group. (D-E)  
1215 Relative abundances (percentage of 16S rRNA gene sequences) of the different  
1216 bacterial families in each sample among the CT, HFD, HFD-CBE, HFD-GPE groups.  
1217 (F) Relative abundances (percentage of 16S rRNA sequences) of the various  
1218 bacterial genera in each sample among each group of mice. Data are presented as  
1219 box-plots. . '\*' and '\*\*' indicate a significant difference versus HFD ( $P<0.05$  and  
1220  $P<0.01$  respectively) as determined by the unpaired two-tailed Student's t-test.

1221

1222 **Figure 7. Effects on intestinal barrier.**

1223 (A-J) qPCR analysis of various markers of the intestinal barrier integrity and  
1224 anti-microbial peptides in the colon (fold change versus CT group). Data are

1225 expressed as mean±s.e.m. Data with different superscript letters are significantly  
1226 different (P<0.05) according to post-hoc one-way ANOVA.

1227

1228

1229 **Figure 8. Effects on bile acids.**

1230 (A) Cecal bile acid concentration (pM/mg cecal content) and percentages of (B)  
1231 conjugated and (C) unconjugated bile acids. (D) Cecal bile acids content (% of  
1232 total bile acids). (E) Plasma bile acid concentrations (nM) and percentages of (F)  
1233 conjugated and (G) unconjugated bile acids. (H) Plasma bile acids content (% of  
1234 total bile acids). (CA: cholic acid; LCA: lithocholic acid; UDCA: ursodeoxycholic  
1235 acid; CDCA: chenodeoxycholic acid; DCA: deoxycholic acid; MCA: muricholic acid;  
1236 T: taurine-; o: omega; a: alpha; b: beta conjugated species). Data are expressed as  
1237 mean±s.e.m. Data with different superscript letters are significantly different  
1238 (P<0.05) according to post-hoc one-way ANOVA.

1239

1240 **Figure 9. Bile acid production**

1241 qPCR analysis of bile acid production/signaling markers: (A) Cyp7a1, (B)  
1242 Cyp7b1, (C) Cyp8a1, (D) cyp27a1, (E) FXR, (F) FGFR4 in the liver. (G) FXR and  
1243 (H) FGF15 in the ileum. Data are expressed as mean±s.e.m. Data with different  
1244 superscript letters are significantly different (P<0.05) according to post-hoc one-  
1245 way ANOVA.

1246

1247 **Figure 10. Cecal short-chain fatty acids (SCFA)**

1248 Concentration of (A) Total short-chain fatty acids (SCFA) content and (B) iso-  
1249 SCFA in the caecum (µmol/g cecal content). (C) mRNA levels of the butyrate  
1250 transporter SLC5a8 in the colon. (D) Relative concentrations of Acetate, Butyrate  
1251 and Propionate (% of total SCFA). Data are expressed as mean±s.e.m. Data with  
1252 different superscript letters are significantly different (P<0.05) according to  
1253 post-hoc one-way ANOVA.

1254

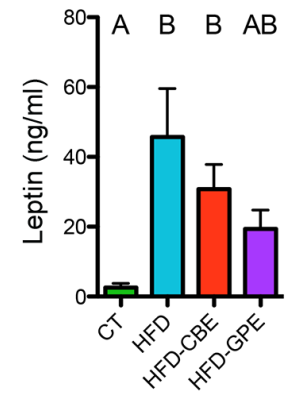
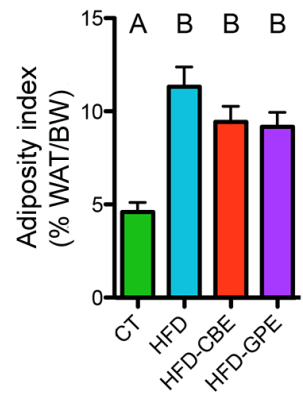
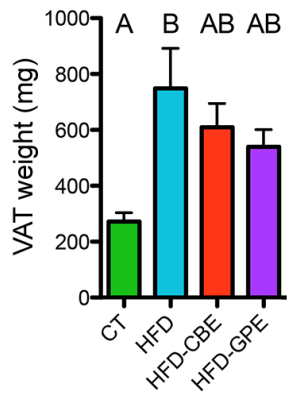
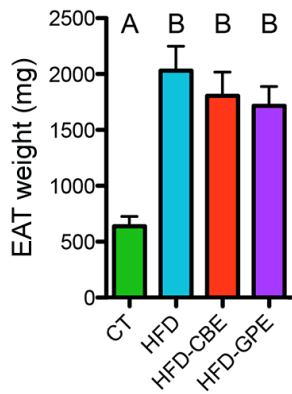
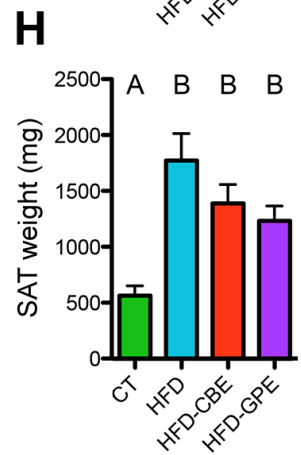
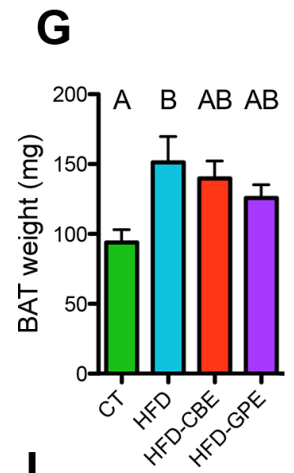
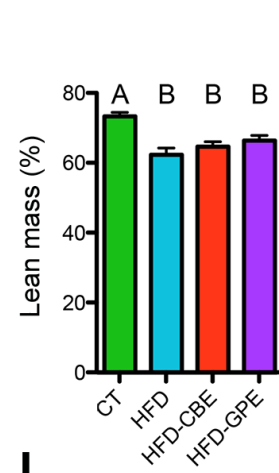
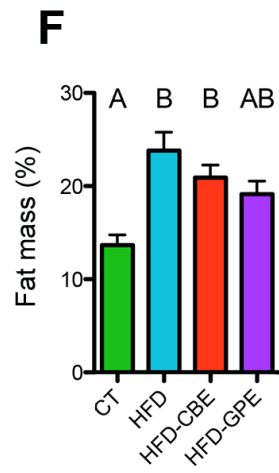
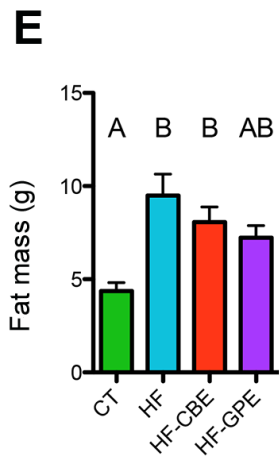
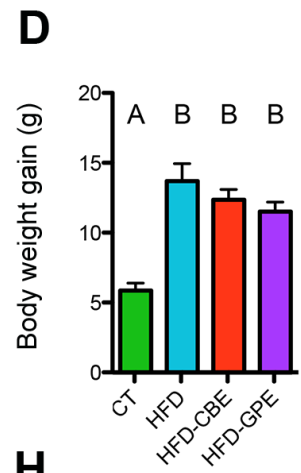
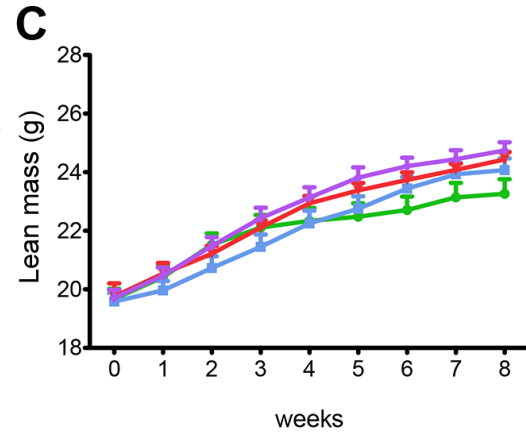
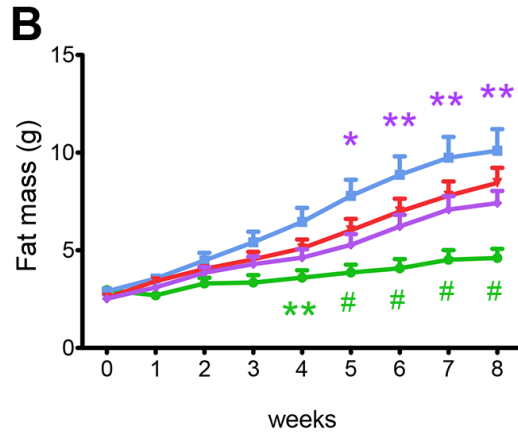
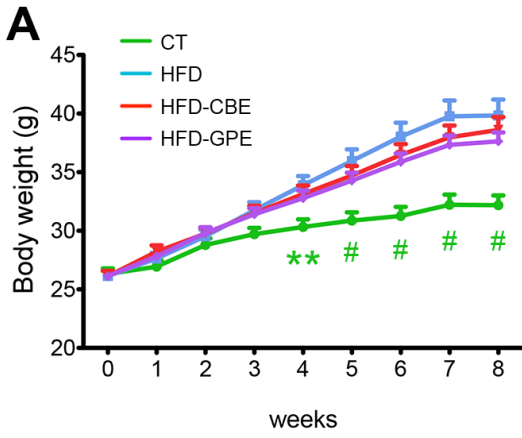
1255 **Table 1**

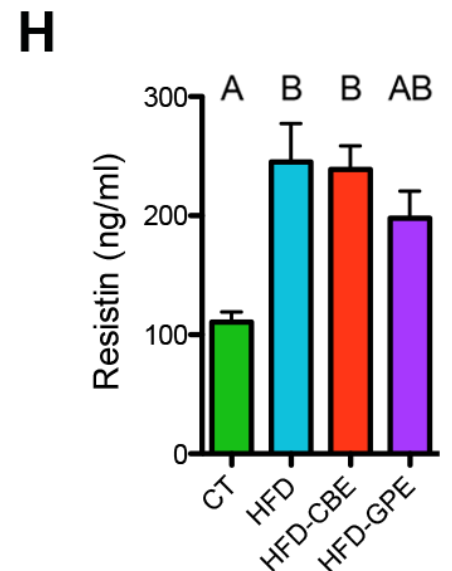
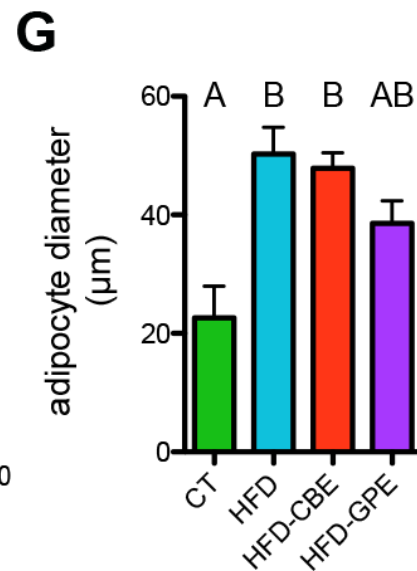
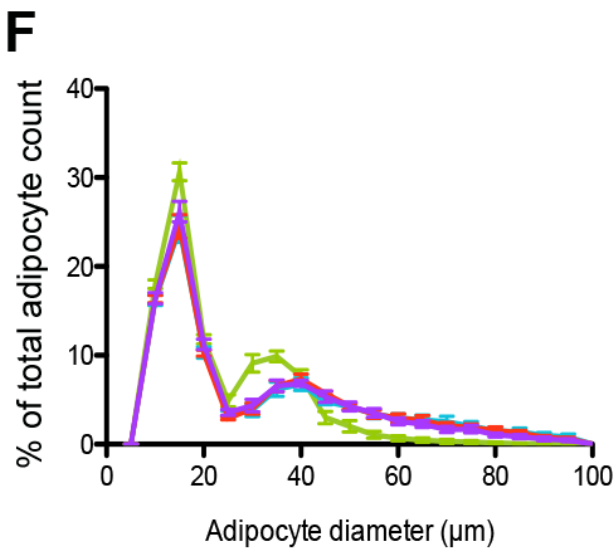
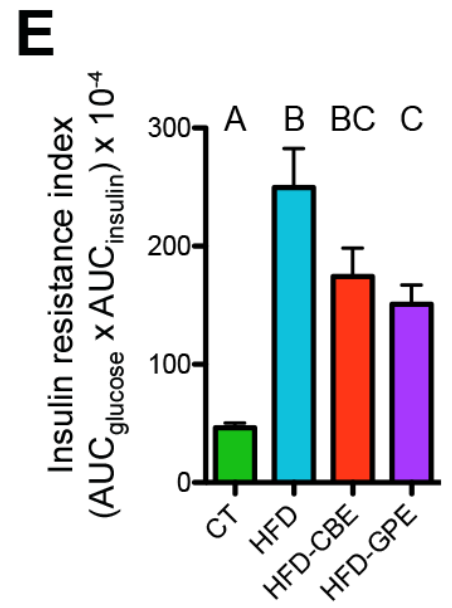
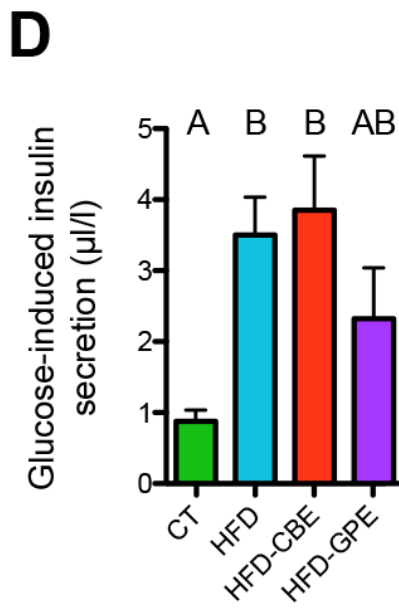
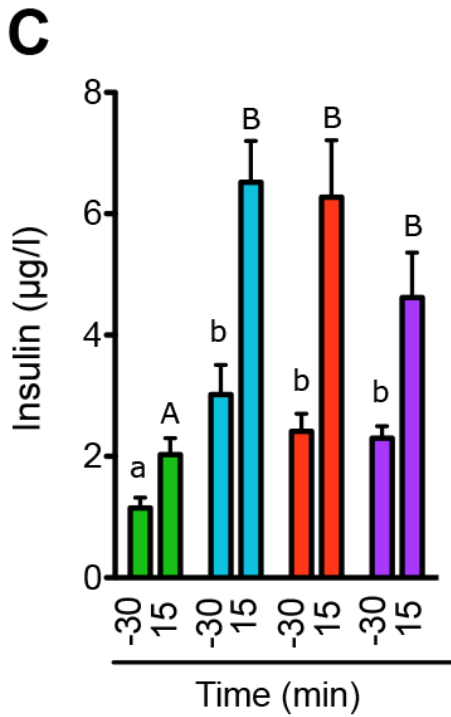
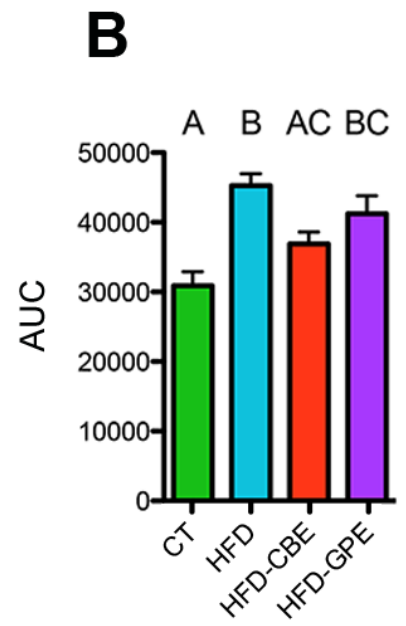
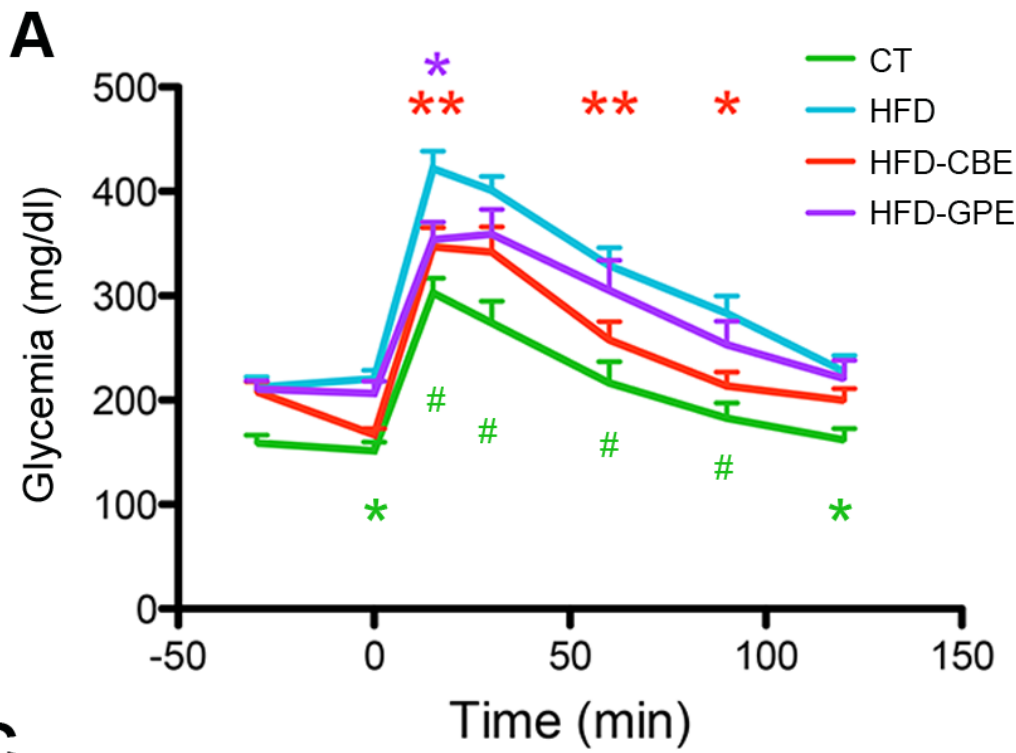
1256 qPCR primer sequences for the targeted mouse genes.

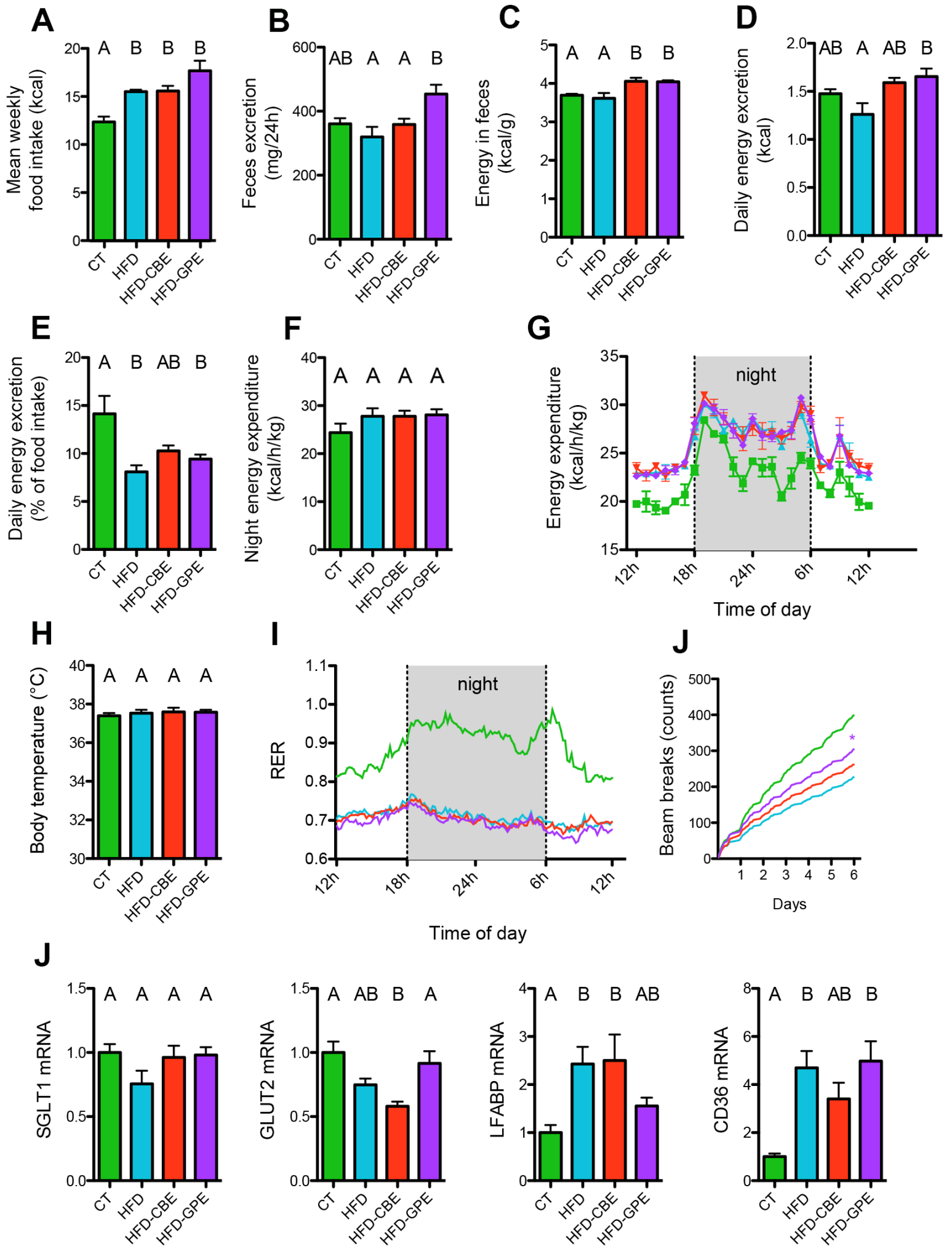
1257

1258 **Table 2**

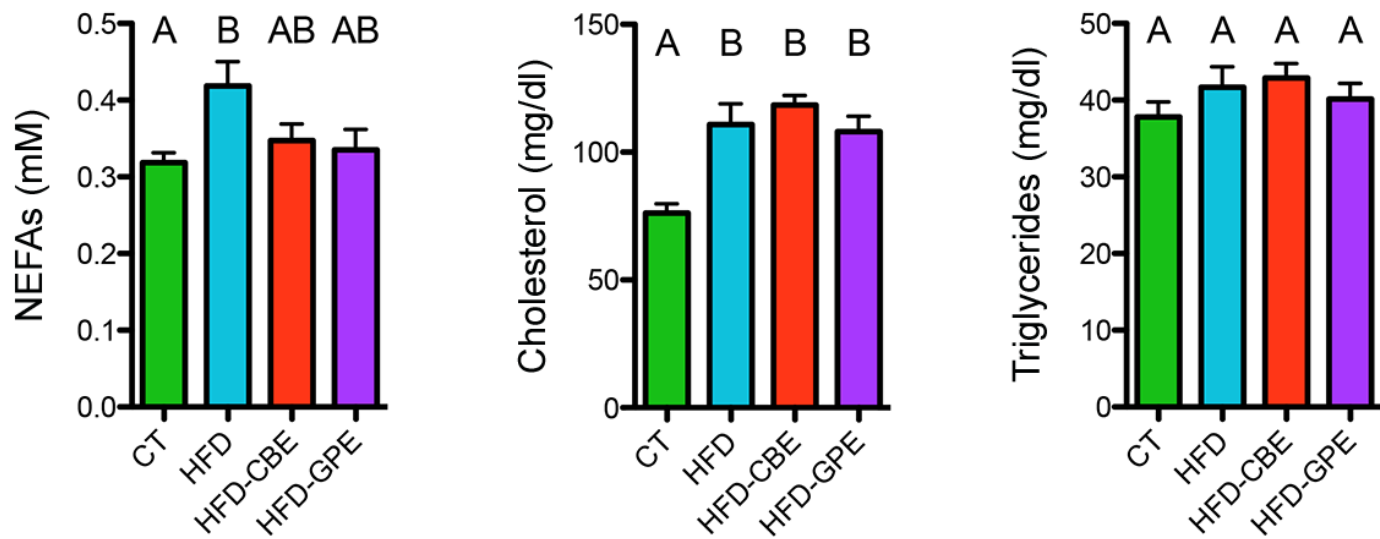
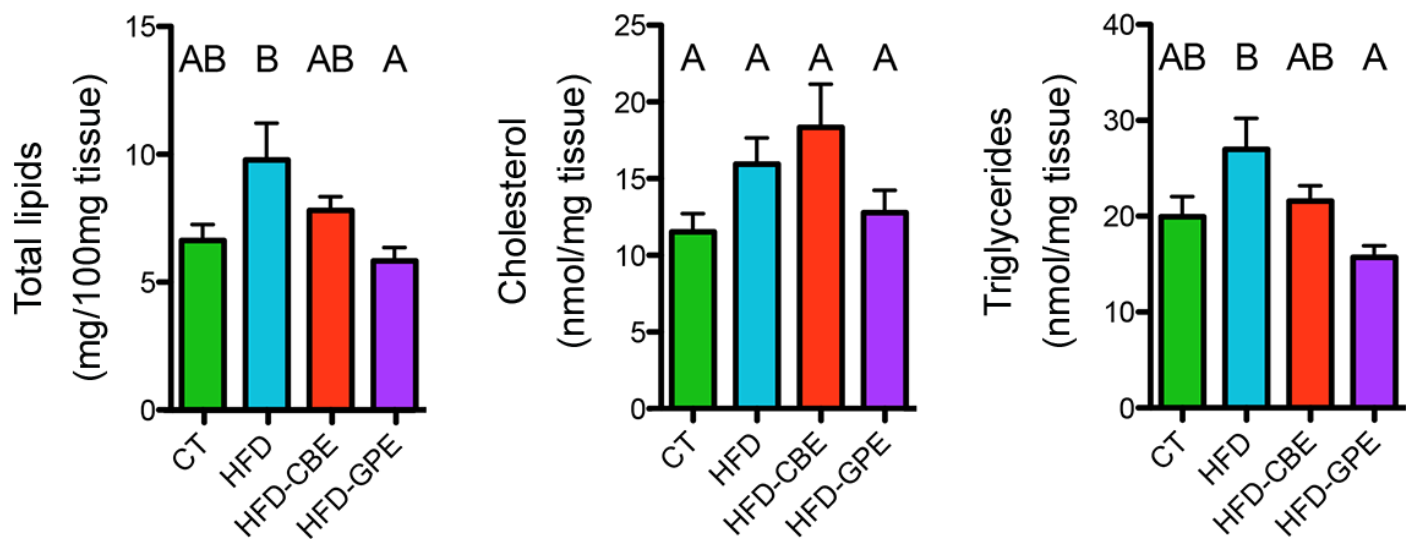
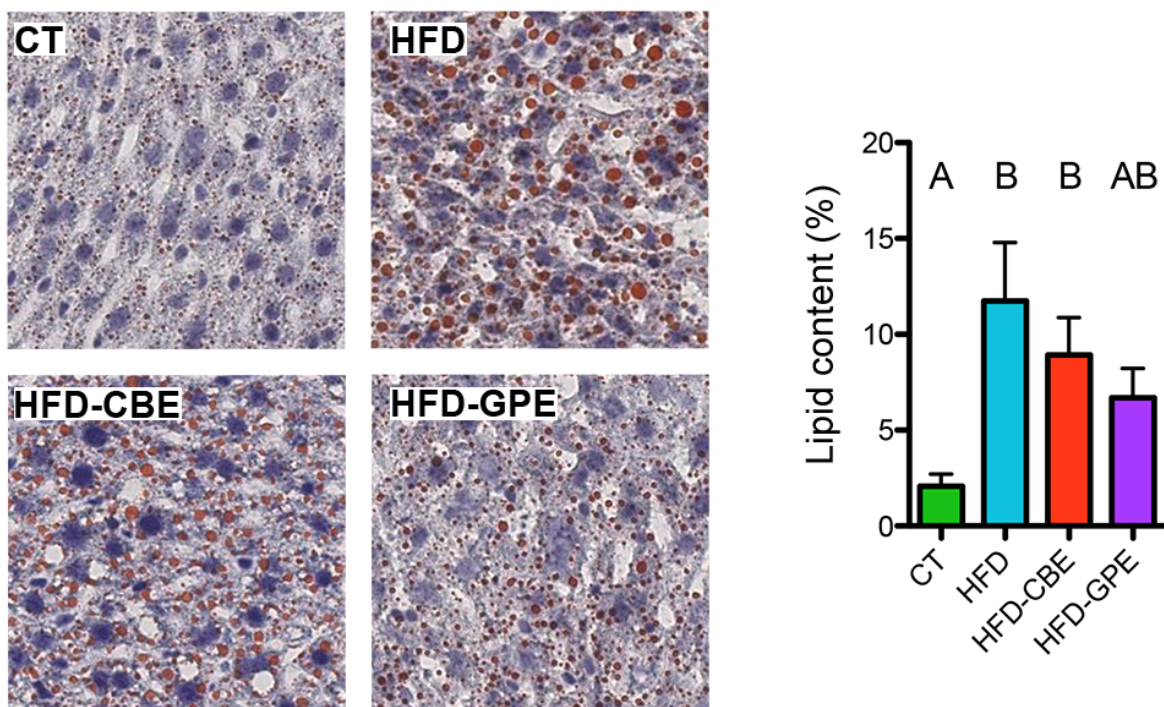
1259 Concentrations of the main components of grape pomace extract and cinnamon  
1260 extract.

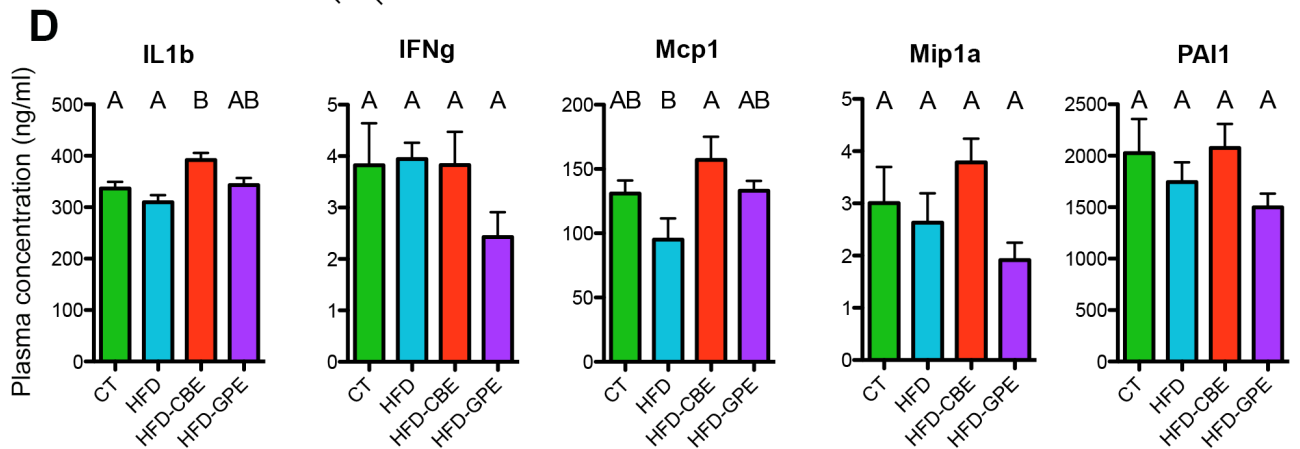
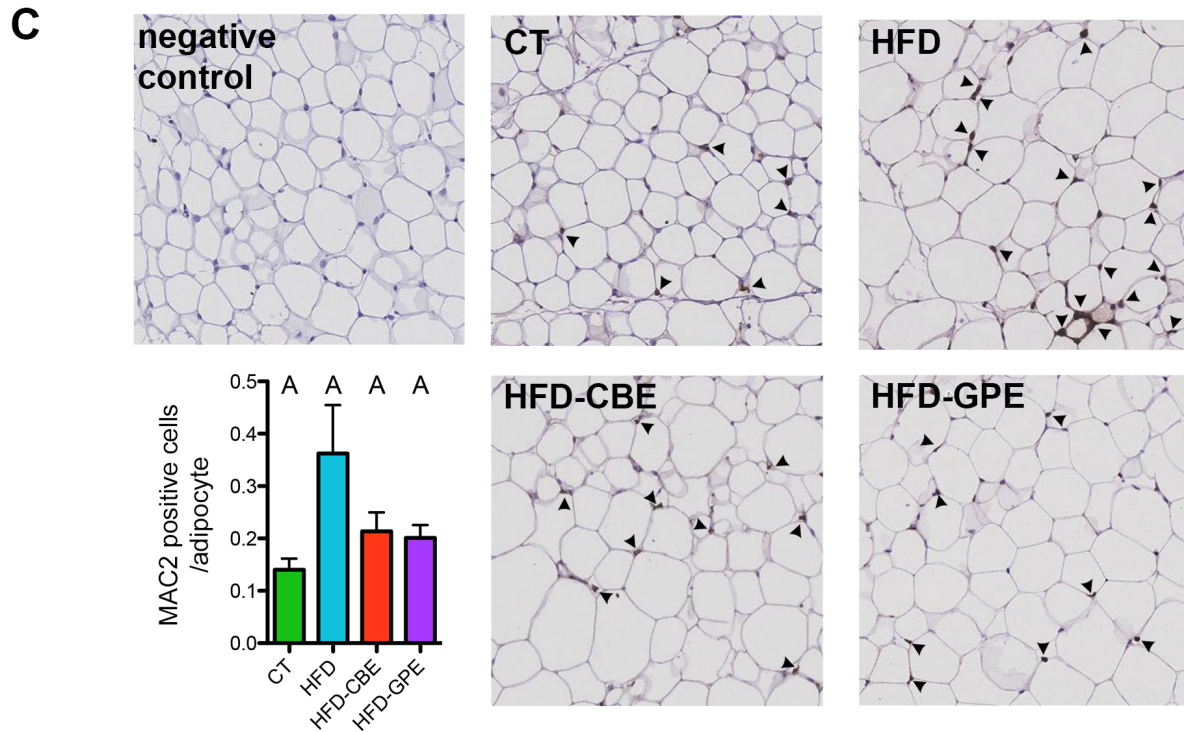
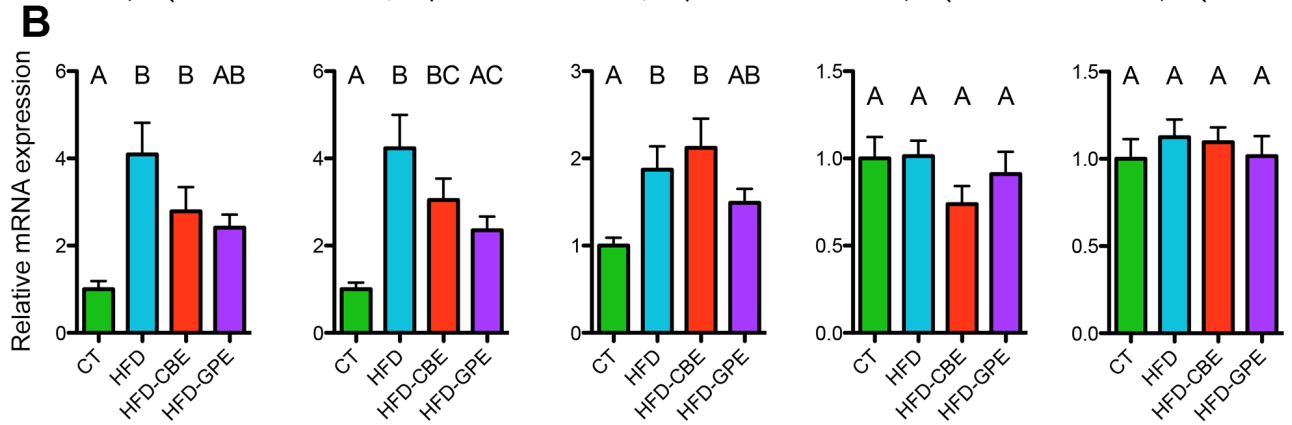
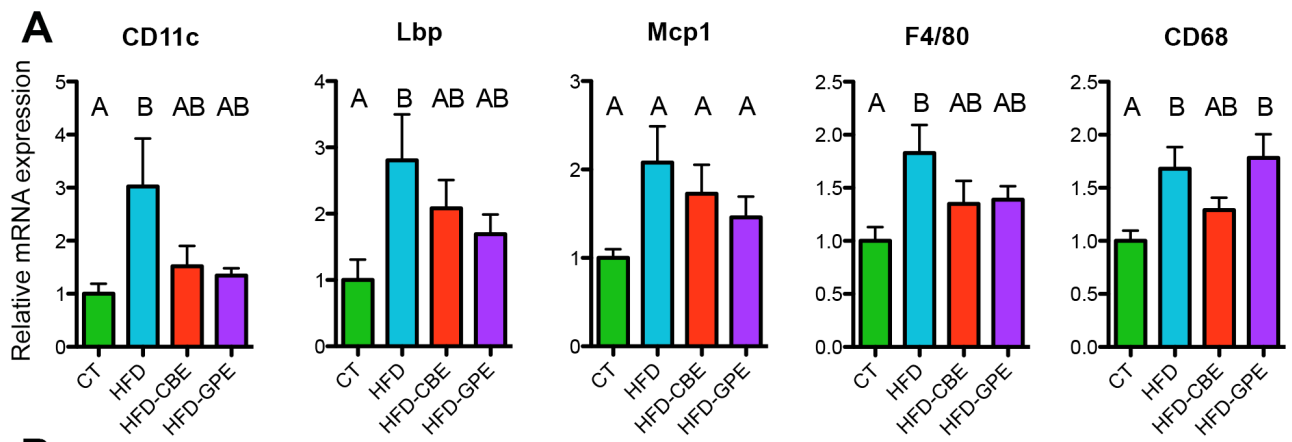




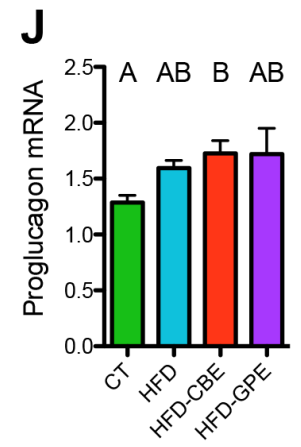
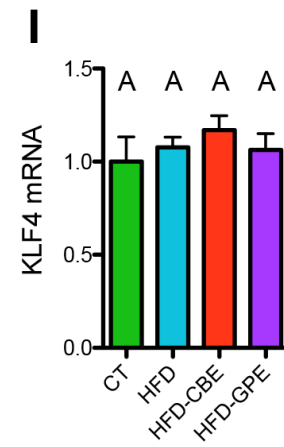
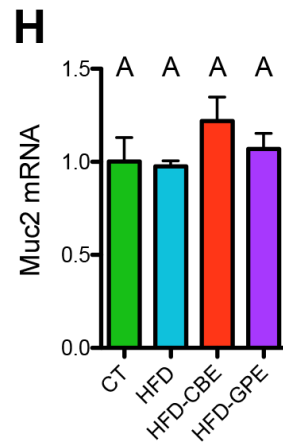
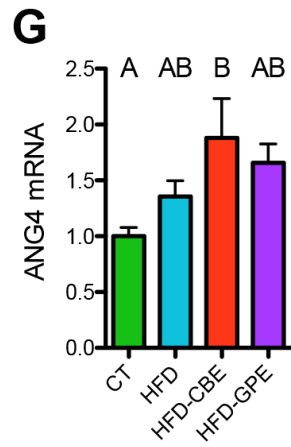
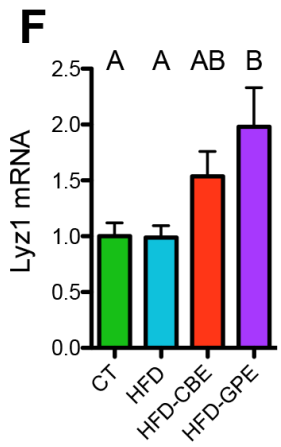
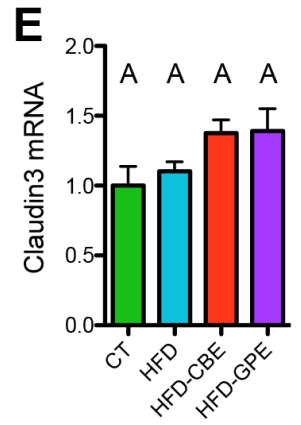
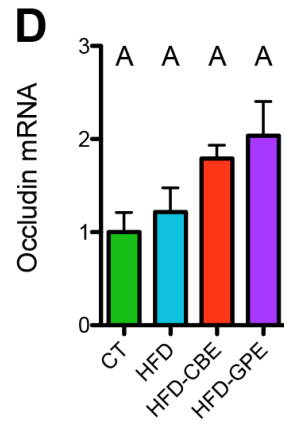
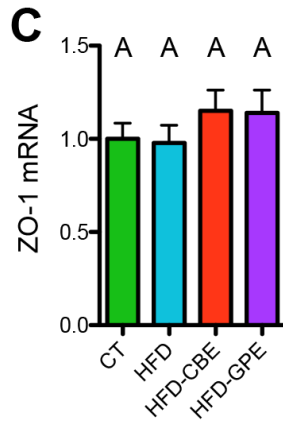
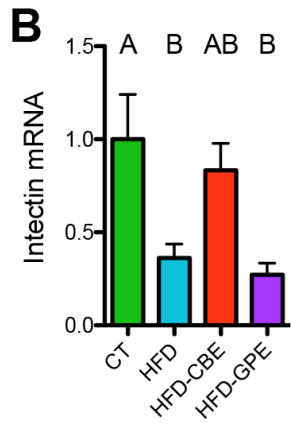
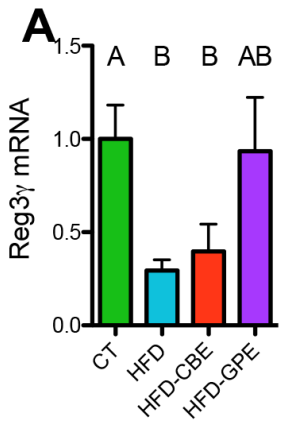




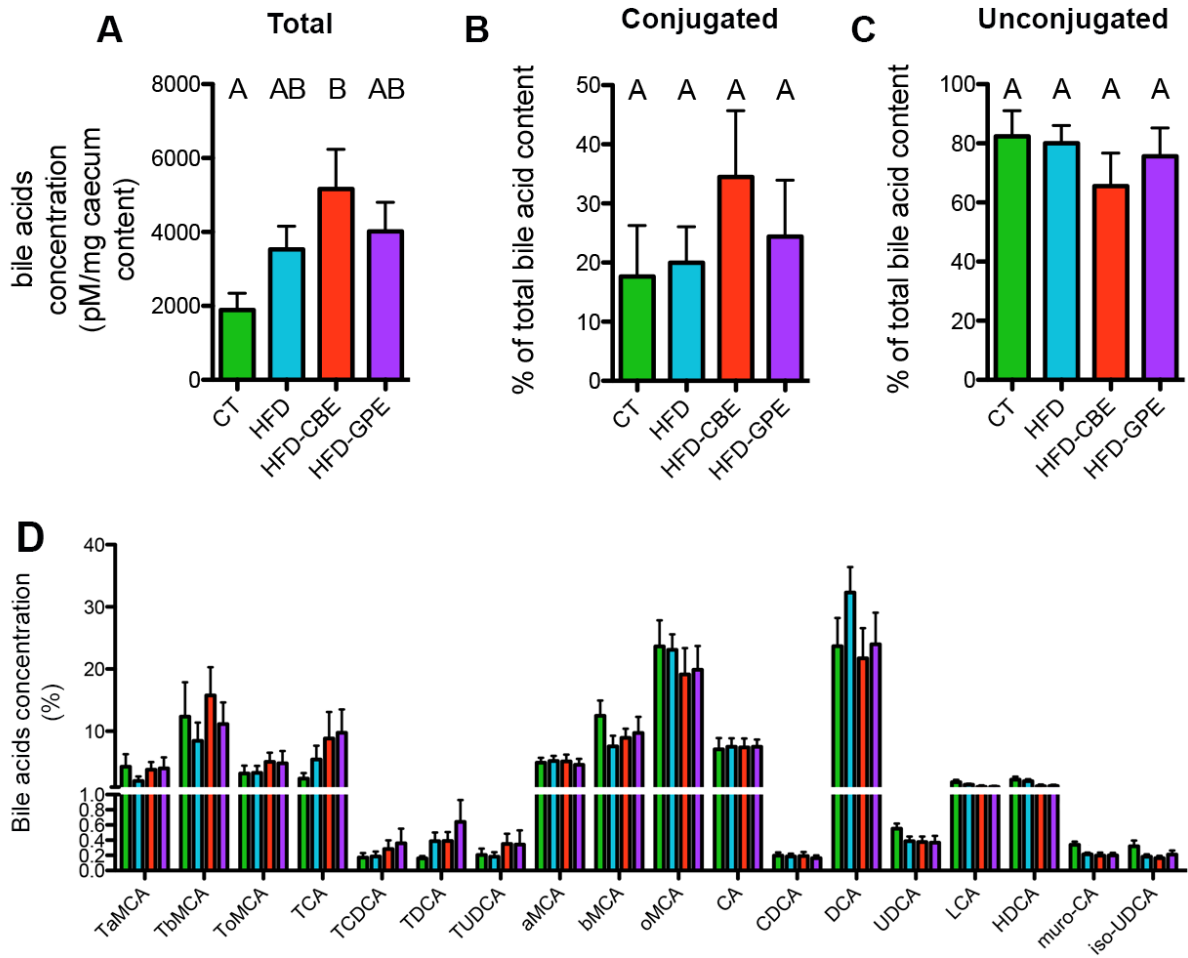
**A****B****C**



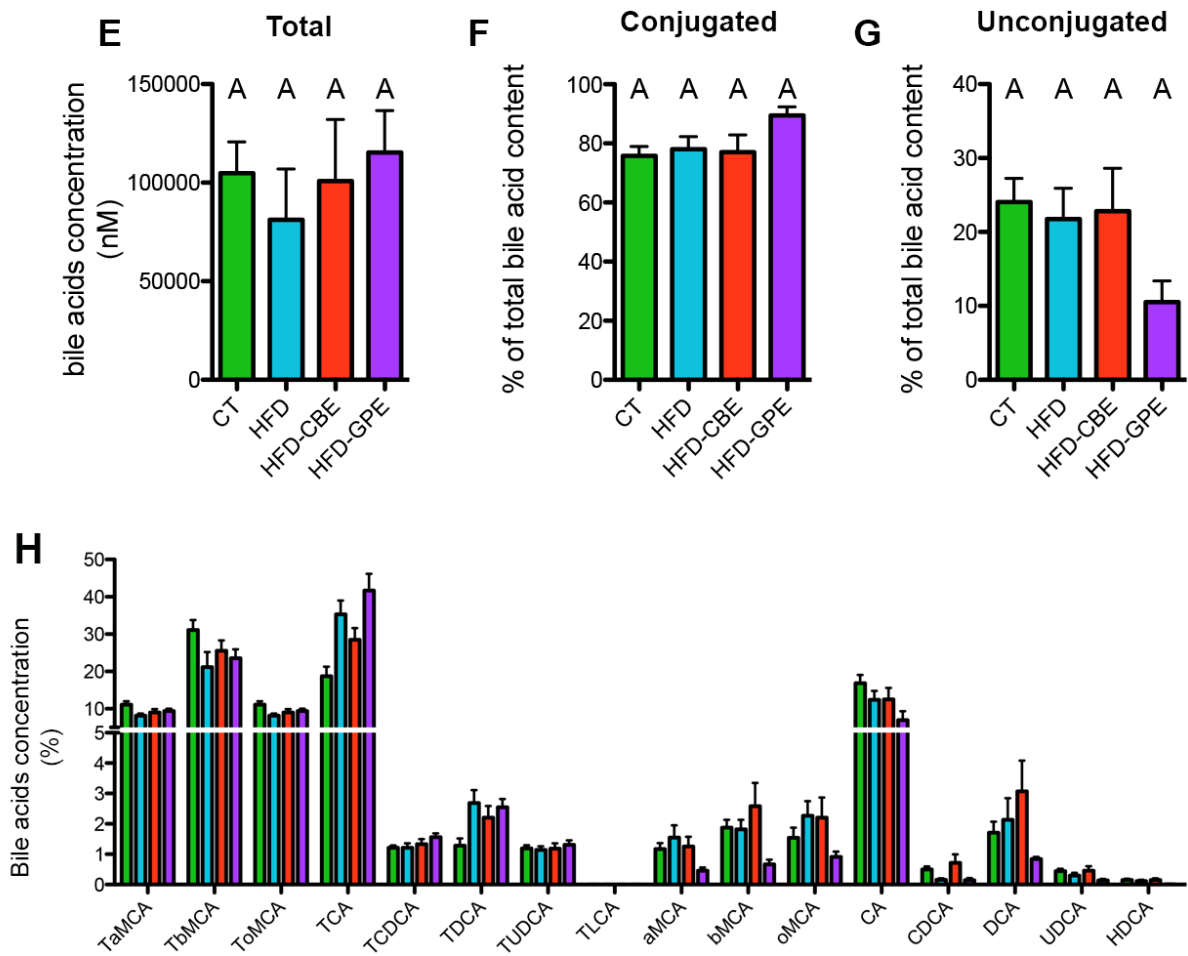


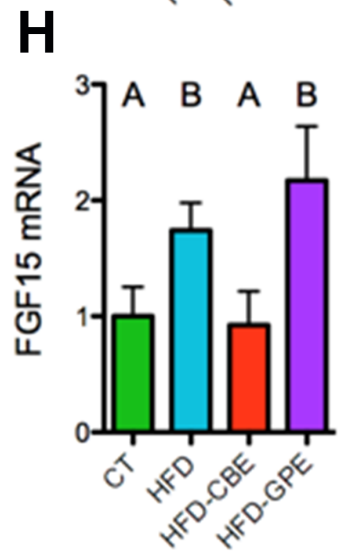
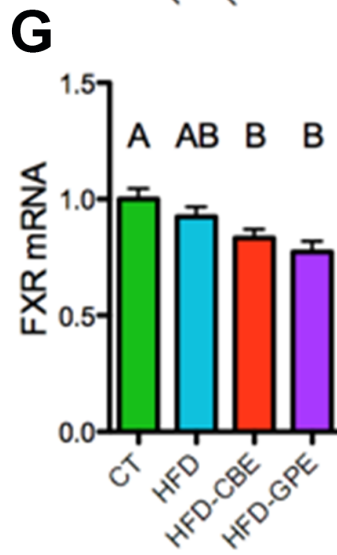
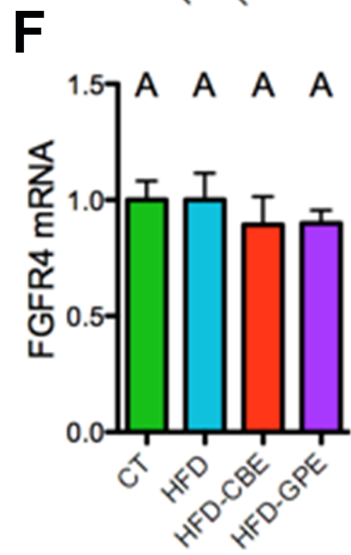
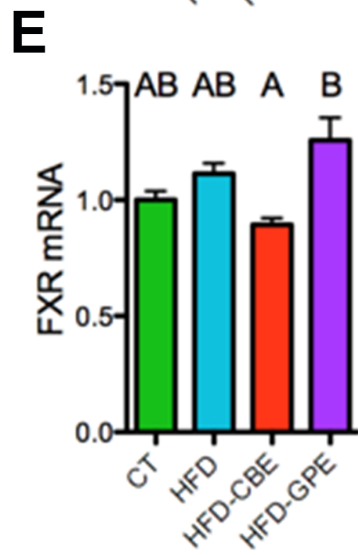
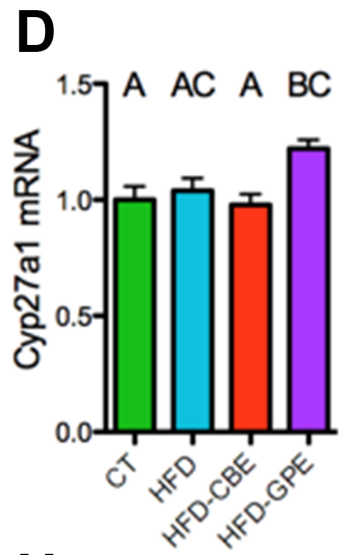
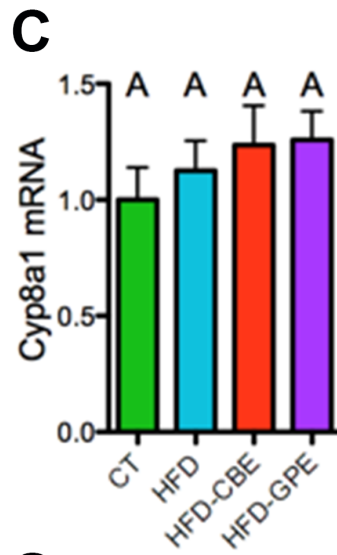
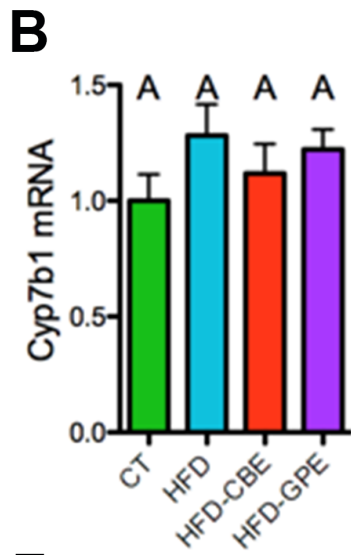
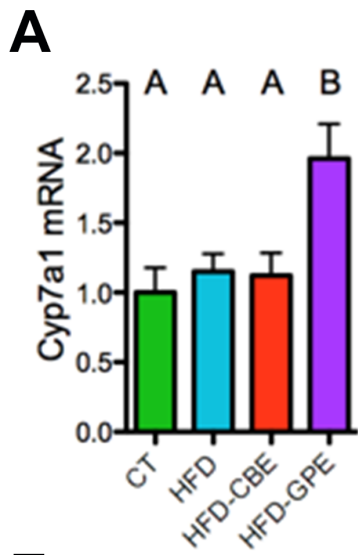


# Caecum

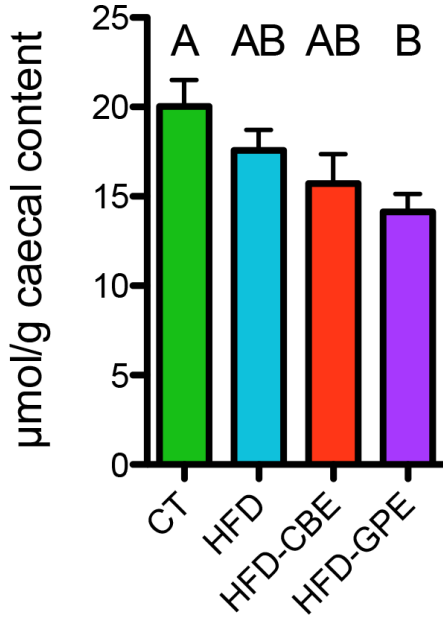


# Plasma

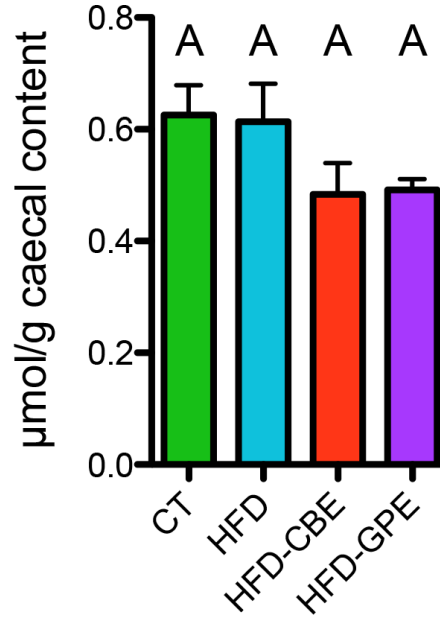




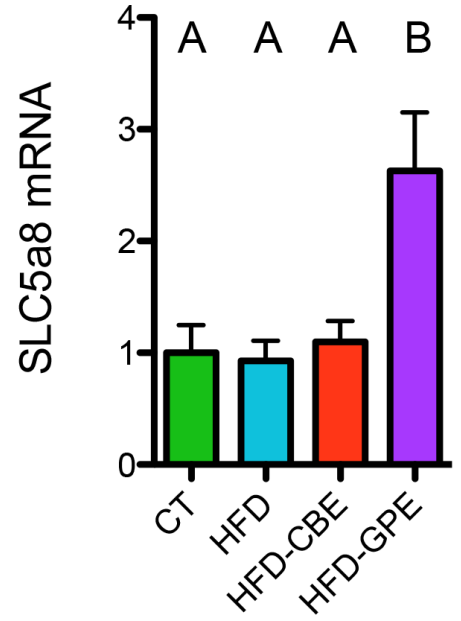
### A Total SCFA



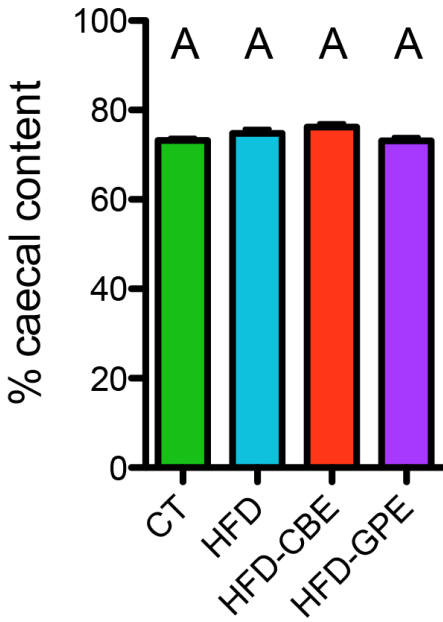
### B Iso-SCFA



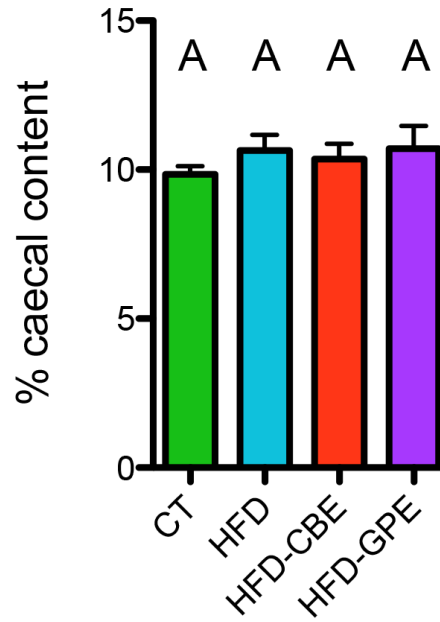
### C SLC5a8 mRNA



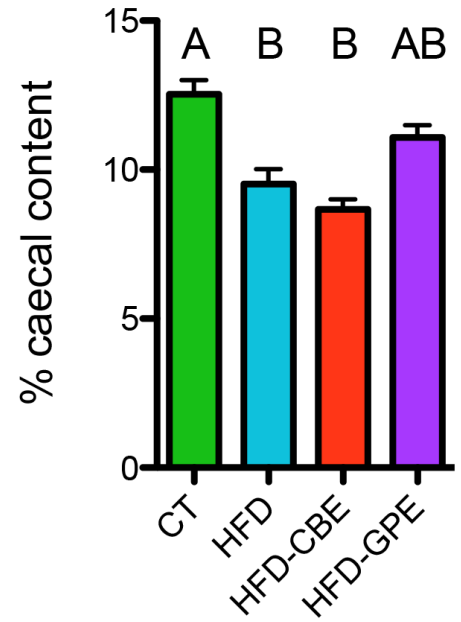
### D Acetate



### Butyrate



### Propionate



| Primers     | Forward Sequence            | Reverse Sequence           |
|-------------|-----------------------------|----------------------------|
| Rpl19       | GAAGGTCAAAGGGAATGTGTTCA     | CCTGTTGCTCACTTGT           |
| Cd11c       | ACGTCAGTACAAGGAGATGTTGGA    | ATCCTATTGCAGAATGCTTCTTTACC |
| Mcp1        | GCAGTTAACGCCCCACTCA         | CCCAGCCTACTCATTGGGATCA     |
| Lbp         | GTCCTGGGAATCTGTCCTTG        | CCGGTAACCTTGCTGTTGTT       |
| Cd68        | CTTCCCACAGGCAGCACAG         | AATGATGAGAGGCAGCAAGAGG     |
| F4/80       | TGACAACCAGACGGCTTG          | GCAGGCGAGGAAAAGATAGTGT     |
| Reg3g       | TTCCTGTCCTCCATGATCAAA       | CATCCACCTCTGTTGGGTTCC      |
| Intectin    | GTTGCCCTGATTCTGCTGG         | GCACTATTGCAGAGGTCC-GT      |
| ZO-1        | TTTTTGACAGGGGGAGTGG         | TGCTGCAGAGGTCAAAGTTCAAG    |
| Occludin    | ATGTCCGGCCGATGCTCTC         | TTTGGCTGCTCTTGGGTCTGTAT    |
| Claudin3    | TCATCGGCAGCAGCATCATCAC      | ACGATGGTGATCTTGGCCTTGG     |
| Lyz1        | GCCAAGGTCTACAATCGTTGTGAGTTG | CAGTCAGCCAGCTTGACACCACG    |
| Ang 4       | CTCTGGCTCAGAATGTAAGGTACGA   | GAAATCTTTAAAGGCTCGGTACCC   |
| Muc2        | ATGCCACCTCCTCAAAGAC         | GTAGTTTCCGTTGGAACAGTGAA    |
| Klf4        | AGAGGAGCCCAAGCCAAAGAGG      | CCACAGCCGTCACAGTCACAGT     |
| Proglucagon | TGGCAGCACGCCCTTC            | GCGCTTCTGTCTGGGA           |
| CYP7a1      | GGGATTGCTGTGGTAGTGAGC       | GGTATGGAATCAACCCGTTGTC     |
| CYP7b1      | TAGGCATGACGATCCTGAAA        | TCTCTGGTGAAGTGGACTGAAA     |
| CYP8a1      | GATCCGTCGCGGAGATAAGG        | CGGGTTGAGGAACCGATCAT       |
| CYP27a1     | TCTGGCTACCTGCACTTCTC        | GTGTGTTGGATGTCGTGTCC       |
| FXR         | TGGGTACCAGGGAGAGACTG        | GTGAGCGCGTTGTAGTGGTA       |
| FGFR4       | CTCGATCCGCTTTGGGAATTC       | CAGGTCTGCCAAATCCTTGTC      |
| FGF15       | GAGGACAAAACGAACGAAATT       | ACGTCCTTGATGGCAATCG        |
| SGLT1       | TCTGTAGTGGCAAGGGGAAG        | ACAGGGCTTCTGTGTCTTGG       |
| GLUT2       | CTGGGTCTGCAATTTTGTC         | TGTAACAGGGTGAAGACCA        |
| LFABP       | ACCTCATCCAGAAAGGGAAGG       | ACAATGTGCCCAATGTCATG       |
| CD36        | GCCAAGCTATTGCGACATGA        | ATCTCAATGTCCGAGACTTTTCAAC  |
| SLC5a8      | GCATATTCGGCATGGTTGGT        | GGGCTCCAATTCCTACCCAT       |

Comment citer ce document :

Van Hul, M., Geurts, Plovier, Druart, Everard, A., Ståhlman, M., Rhimi, M., Chira, K., Teissedre, P. L., Delzenne, Maguin, E., Guilbot, A., Brochot, A. (Co-dernier auteur), Gérard, P. (Co-dernier auteur), Bäckhed, F. (Co-dernier auteur), Cani, P. D. (Auteur de correspondance) (2018). Reduced obesity, diabetes and steatosis upon cinnamon and grape pomace are associated with



Table 2. Concentrations of the main components of grape pomace extract and cinnamon extract.

| <b>Main tannin concentrations in GPE (mg/g of the extract)</b> |                            |                          |
|--|----------------------------|--------------------------|
|  | <b>mg/g of the extract</b> | <b>Daily dose (ng/d)</b> |
| Catechin   | 1.732 ± 0.089              | 48,40 ± 3,23             |
| Procyanidin B1 dimer   | 0.100 ± 0.011              | 2,79 ± 0,18              |
| Procyanidin B2 dimer   | 0.311 ± 0.032              | 8,69 ± 0,58              |
| Procyanidin B3 dimer   | 0.350 ± 0.022              | 9,78 ± 0,65              |
| Procyanidin B4 dimer   | 0.090 ± 0.001              | 2,51 ± 0,16              |
| Procyanidin C2 trimer  | 0.071 ± 0.001              | 1,98 ± 0,13              |
| Epicatechin  | 1.011 ± 0.045              | 28,25 ± 1,88             |
| Total tanins   | 3.66 ± 0.625               | 102,27 ± 6,83            |

| <b>Main anthocyanins concentrations in GPE</b> |                            |                          |
|--|----------------------------|--------------------------|
|  | <b>mg/g of the extract</b> | <b>Daily dose (ng/d)</b> |
| Delphinidin-3-O-glucoside                      | 1.635 ± 0.016              | 45,69 ± 3,05             |
| Cyanidin-3-O-glucoside                         | 0.513 ± 0.007              | 14,33 ± 0,95             |
| Petunidin-3-O-glucoside                        | 2.744 ± 0.027              | 76,67 ± 5,12             |
| Peonidin-3-O-glucoside                         | 8.687 ± 0.258              | 242,74 ± 16,21           |
| Malvidin-3-O-glucoside                         | 21.594 ± 0.213             | 603,39 ± 40,3            |
| Peonidin-3-O-(6'' acetyl-glucoside)            | 0.546 ± 0.003              | 15,26 ± 1,02             |
| Malvidin-3-O-(6'' acetyl-glucoside)            | 1.476 ± 0.026              | 41,24 ± 2,75             |
| Peonidin-3-O-(6''-p-coumaryl-glucoside)        | 1.596 ± 0.018              | 44,6 ± 2,98              |
| Malvidin-3-O-(6''-p-coumaryl-glucoside)        | 4.624 ± 0.012              | 129,21 ± 8,63            |
| Total anthocyanins                             | 43.416 ± 6.793             | 1213,15 ± 81,03          |

| <b>Phenolic composition of GPE</b> |                            |                          |
|------------------------------------|----------------------------|--------------------------|
|                                    | <b>mg/g of the extract</b> | <b>Daily dose (ng/d)</b> |
| Total phenolics (1)                | 82.663 ± 2.534             | 2309,81 ± 154,28         |
| Total anthocyanins (2)             | 43.969 ± 3.497             | 1228,6 ± 82,06           |
| Total tanins (3)                   | 26.006 ± 1.066             | 726,67 ± 48,54           |

(1) Total phenolics, mg/g as gallic acid equivalent (Folin Ciocalteu assay)

(2) Total anthocyanins, mg/g as cyanidin-3-O- glucoside equivalent

(3) Total tanins, mg/g as procyanidin B2 equivalent (Bate-Smith assay)

| <b>Main components in CBE</b> |                            |                          |
|-------------------------------|----------------------------|--------------------------|
|                               | <b>mg/g of the extract</b> | <b>Daily dose (ng/d)</b> |
| Total polyphenols             | 79                         | 1174,45 ± 40,46          |
| Proanthocyanidin A            | 90                         | 1337,99 ± 46,09          |
| Coumarin                      | 9                          | 133,8 ± 4,609            |
| Cinnamaldehyde                | 1,8                        | 26,76 ± 0,92             |
| Eucalyptol                    | not detected               |                          |

Comment citer ce document :

Van Hul, M., Geurts, Plovier, Druart, Everard, A., Ståhlman, M., Rhimi, M., Chira, K., Teissedre, P. L., Delzenne, Maguin, E., Guilbot, A., Brochot, A. (Co-dernier auteur), Gérard, P. (Co-dernier auteur), Bäckhed, F. (Co-dernier auteur), Cani, P. D. (Auteur de correspondance) (2018). Reduced obesity, diabetes and steatosis upon cinnamon and grape pomace are associated with